POLITECNICO DI TORINO
Repository ISTITUZIONALE

Traffic-induced atmospheric pollution during the COVID-19 lockdown: Dispersion modeling based on traffic flow monitoring in Turin, Italy
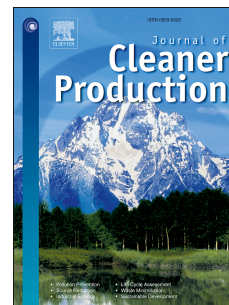
(Article begins on next page)

07 May 2024

Journal Pre-proof

Traffic-induced atmospheric pollution during the COVID-19 lockdown: Dispersion modeling based on traffic flow monitoring in Turin, Italy

Marco Ravina, Zahra Shams Esfandabadi, Deborah Panepinto, Maria Chiara Zanetti

Please cite this article as: Ravina M, Esfandabadi ZS, Panepinto D, Zanetti MC, Traffic-induced atmospheric pollution during the COVID-19 lockdown: Dispersion modeling based on traffic flow monitoring in Turin, Italy, *Journal of Cleaner Production* (2021), doi: https://doi.org/10.1016/j.jclepro.2021.128425.

Traffic-induced atmospheric pollution during the COVID-19 lockdown: dispersion modeling based on traffic flow monitoring in Turin, Italy

Marco Ravina*,[1], Zahra Shams Esfandabadi[1,2], Deborah Panepinto[1], Maria Chiara Zanetti[1]

[1] Department of Environment, Land and Infrastructure Engineering (DIATI), Politecnico di Torino, Corso Duca degli Abruzzi 24, 10129 Torino, Italy

[2] Energy center lab, Politecnico di Torino, Via Paolo Borsellino 38/16, 10138 Torino, Italy

* Corresponding author; Email: Marco.ravina@polito.it

Abstract

The COVID-19 pandemic, as a worldwide threat to public health, has led many governments to impose mobility restrictions and adopt partial or full lockdown strategies in many regions to control the disease outbreak. Although these lockdowns are imposed to save public health by reducing the transmission of the virus, rather significant improvements of the air quality in this period have been reported in different areas, mainly as a result of the reduction in vehicular trips. In this research, the city of Turin in the northern part of Italy has been considered as the study area, because of its special meteorology and geographic location in one of the most polluted regions in

20 Europe, and also its high density of vehicular emissions. A Lagrangian approach is applied to

21 illustrate and analyze the effect of imposing full lockdown restrictions on the reduction of traffic-

22 induced air pollution in the city. To do this, the real-time traffic flow during the lockdown period

23 is recorded, and by utilizing CALPUFF version 7, the dispersion of $PM_{2.5}$, Total Suspended

24 Particulate (TSP), Benzo(a)pyrene (BaP), NO_x, and Black Carbon (BC) emitted from all

25 circulating vehicles during and before the lockdown period are compared. Results indicate that the

26 concentration of pollutants generated by road traffic sources (including passenger cars, busses,

27 heavy-duty vehicles, light-duty vehicles, mopeds, and motorcycles) reduced at least 70% (for

28 $PM_{2.5}$) up to 88.1% (for BaP) during the studied period. Concentration maps show that the

29 concentration reduction varied in different areas of the town, mainly due to the characteristics and

30 strength of the emission sources and the geophysical features of the area.

31 Keywords: Air quality, Dispersion Modeling, Emission, Pandemic, Transportation, Urban

32 planning.

1. Introduction

34   The novel coronavirus-caused infectious disease 2019 (COVID-19), which was announced as

35 a pandemic by the World Health Organization (WHO) on March 11, 2020 (WHO, 2020) has made

36 a shock to the world and is turning into the largest threat to the public health worldwide in the 21st

37 century (Chakraborty and Maity, 2020). To control the disease outbreak and flattening the

38 epidemic curve, many regions have been imposing a partial or full lockdown in the highly infected

39 areas. Although the lockdown restrictions were established to save public health by reducing the

40 transmission of the virus, changes in the air and water quality in some areas (Ambade et al., 2021;

41 Muhammad et al., 2020; Saadat et al., 2020; Sharifi and Khavarian-Garmsir, 2020) have attracted

42 the attention towards the environmental impacts of the pandemic lockdowns globally. In this

43 regard, numerous research has been conducted on the changes in the air quality during the

44 lockdown period in different countries across the globe, from China in the East (Griffith et al.,

45 2020; Huang et al., 2020) to the United States in the West (Naeger and Murphy, 2020; Zangari et

46 al., 2020), and some large areas such as western Europe (Menut et al., 2020). Besides, several

47 pieces of research studied the potential link between the improvements in the air quality as a result

48 of mitigating COVID-19 measures and the health benefits. These studies mainly concluded lower

49 air pollution-related mortality due to less exposure to air pollution during this period (Gupta et al.,

50 2020; Liu et al., 2021; Son et al., 2020). All these studies highlight the importance of air pollution

51 control strategies to protect human health whether air pollutants increase the infection rate of

52 COVID-19 or not (Cazzolla Gatti et al., 2020; Collivignarelli et al., 2021a; Dettori et al., 2020).

53 Air pollution, with its impacts both at the local and global scales, has caused many challenges

54 and problems all around the world over the years (Izquierdo et al., 2020; Sivarethinamohan et al.,

55 2020) such that concerns about this issue have been reflected in the 2030 Agenda for Sustainable

56 Development adopted by the United Nations General Assembly (UN, 2015). The WHO has labeled

57 air pollution as the major environmental threat to health (WHO, 2016) and has estimated that

58 around 90% of the world population do not breathe the air complying with its Air Quality

59 Guideline (WHO, 2005). Exposure to air pollutants leads to three million deaths per year (WHO,

60 2016), out of which 600,000 deaths happen among children less than five years of age (WHO,

61 2017). Such negative health impacts impose substantial economic costs to the societies (Chen and

62 Chen, 2021; Stewart et al., 2017) and affect both humans and ecosystems (Panepinto et al., 2014).

63 Therefore, in order to take steps towards clean air transitions, air quality action plans have been

64 considered as blueprints to achieve certain air quality objectives (Gross et al., 2019) by many

65 countries all around the world, such as Spain (Izquierdo et al., 2020), China (Cai et al., 2017), the

66 United Kingdom and the United States (Gross et al., 2019).

67 Air quality analysis and modeling in urban areas involve an inherent complexity (Pinto et al.,

68 2020) due to the existence of a high number of air pollutant emission sources, the meteorological

69 conditions of the region affecting the dispersion of the pollutants (Shen et al., 2021) and the

70 chemical transformations of pollutants into secondary aerosols (EPA, 2015). However, air

71 pollution dispersion models provide useful means to support decision-making in air quality control

72 (Holnicki et al., 2016; Ravina et al., 2019) through estimating the concentration of pollutants in

73 the atmosphere (Khan and Hassan, 2020). These deterministic mathematical models mostly follow

74 Gaussian, Eulerian, or Lagrangian approaches (Liu et al., 2019), the Gaussian being a steady-state

75 model and the two others being time-dependent (Khan and Hassan, 2020).

76 Dispersion models have been widely used for modeling the concentration of air pollutants in

77 various case studies. In research conducted by Kesarkar et al. (2007), AERMOD, which is a

78 steady-state Gaussian model, was utilized to model the dispersion of PM_{10} in Pune, India.

79 Modeling the dispersion of PM_{10} was also conducted by Brusca et al. (2016) for the city of Turin,

80 Italy, which is also the case study in the present research, by applying a 3D Computational Fluid

81 Dynamics (CFD), coupling Eulerian and Lagrangian approaches. Omidi Khaniabadi et al. (2018)

82 used the Gaussian SCREEN3 model and a Gaussian plume model to investigate the dispersion of

83 fine particles including PM_{10}, $PM_{2.5,}$ and $PM_{1.0}$ related to a cement plant in Iran. Abdul-Wahab et

84 al. (2017) considered a cement plant in Oman and used CALPUFF, as an advanced non-steady-

85 state Lagrangian puff model, to model the dispersion of CO_2 emission. Moreover, Ravina et al.

4

86   (2018) used CALPUFF as a part of an integrated dispersion and externalities model to estimate

87   the delta-concentration maps for NOx, $PM_{2.5,}$ and PM_{10} and calculate the health damage costs for

88   the district heating system in the city of Turin. Selection among CALPUFF, SPRAY (which is a

89   Lagrangian particle model), and AERMOD for modeling the pollutant dispersion is possible in the

90   extended version of this integrated model (Ravina et al., 2020b).

91   Air pollution in urban areas is mainly linked with vehicular trips (Guttikunda et al., 2019; Pinto

92   et al., 2020; Xiang et al., 2020). Therefore, the travel of various types of vehicles with different

93   ages and fuel types on urban roads and streets adds more complication to the inherent complexity

94   of the air quality modeling. However, air pollution dispersion models have also been used in the

95   literature with a focus on traffic-induced air pollution. For instance, in the Tehran Metropolitan in

96   Iran, which is struggling with air pollution as a major problem, Shahbazi et al. (2017) studied the

97   impact of the traffic emission reduction plans on the concentration of CO and NO_x in the city by

98   using Comprehensive Air Quality Model with Extensions (CAMx) that is an Eulerian

99   photochemical model. Also, Shahbazi and Hosseini (2020) used CAMx to investigate the

100   concentration of CO, NO_2, O_3, $PM_{2.5}$, SO_2, and Black Carbon (BC) in Tehran in a highly polluted

101   period in December 2017. Furthermore, considering the high level of traffic-related pollution in

102   the metropolitan area of Madrid, Spain, and the Air Quality and Climate Change Plan launched by

103   the city council to tackle air pollution issues, Izquierdo et al. (2020) used an Eulerian chemical-

104   transport model called Community Multiscale Air Quality (CMAQ) to evaluate the outcome of

105   implementing this plan regarding the concentration levels of $PM_{2.5}$, NO_2 and O_3 in the city. In

106   another research, Borge et al. (2018) also used CMAQ to assess the traffic-related NO_2 emissions

107   based on a short-term action plan in the city of Madrid. Applying CALPUFF, Abdul-Wahab and

108   Fadlallah (2014) and Charabi et al. (2018) studied the concentration of CO, NOx, and CO_2

109   resulting from traffic in two different areas in Oman.

110   The lockdowns imposed by the governments to control the spread of COVID-19 highly

111   impacted the transportation sector in all countries (Gualtieri et al., 2020; Ranjbari et al., 2021), and

112   therefore, rather significant improvements in the air quality in this period have been reported in

113   many areas (Chen et al., 2021; Gautam, 2020; Wang et al., 2020; Xiang et al., 2020). However, Le

114   et al. (2020) highlighted the unexpected air pollution in northern China during the COVID-19

115   lockdown period, which happened despite up to 90% reduction of certain emissions from various

116   sources in this period. Improvements in the air quality have also been observed in Italy (Deserti et

117   al., 2020a, 2020b), with an average of 48-60% reduction in road traffic leading to a significant

118   reduction in NO_2 levels (Gualtieri et al., 2020). Collivignarelli et al. (2021b) studied the impact of

119   the pandemic on the concentration of NO_2 in three megacities of London, Milan, and Paris,

120   highlighting the role of traffic restrictions on the reduction of NO_2 concentration in these cities.

121   Although Xiang et al. (2020) showed that considering meteorological conditions plays a

122   significant role in concluding the impacts of the pandemic on the traffic-induced air pollution

123   levels within the cities, to the best of the authors' knowledge, no study has utilized air pollution

124   dispersion models to study the changes in the concentration of air pollutants during the COVID-

125   19 pandemic lockdown mainly focusing on the changes in urban transportation activities, yet. This

126   is while some pieces of research are available on the analysis of the impact of COVID-19

127   restrictions on the changes in the traffic-related air pollution considering meteorological conditions

128   from the lens of statistical analysis (Chen et al., 2021; Rossi et al., 2020; Xiang et al., 2020).

129   Furthermore, as stated by Gualtieri et al. (2020), most of the studies focusing on the implications

130   of COVID-19 lockdowns for the urban air quality lack quantification of the changes in road mobile

131   sources during the lockdown restrictions.

132   Therefore, to fill the existing gap, the present research aims at applying a Lagrangian approach

133   to illustrate and analyze the role of traffic in the city of Turin, Italy, on the air quality of the city

134   during the lockdown period. This is done by comparing the emission of NO_2, Benzo(a)pyrene

135   (BaP), $PM_{2.5}$, Total Suspended Particulate (TSP), and BC from all traffic mobile sources in the

136   city during normal days and the COVID-19 country lockdown period based on the real-time traffic

137   flow data recorded in this period. Since the first pandemic lockdown and mobility restrictions in

138   Italy led to 42% fewer daily trips (Cartenì et al., 2020), modeling the dispersion of traffic-induced

139   pollutants before and during the lockdown period can provide useful insight into the role of mostly

140   unnecessary traffic in polluting the atmosphere in this city.

141   The remainder of the paper is structured as follows. Section 2 introduces the study area and

142   provides an overview of the research method applied, and the data gathered. Sections 3 presents

143   the results and section 4 provides a discussion and analysis on the maps illustrating the

144   concentration of pollutants before and during the lockdown period. Finally, section 5 concludes

145   the key findings of the paper on the changes in the concentration of air pollutants during the

146   COVID-19 pandemic lockdown, which are attributed to the changes in vehicular transportation

147   activities.

148

2. Materials and Method

2.1. Description of the study area

This research considers the city of Turin as the study area for two main reasons: (1) its special meteorological and geographic condition in Po Valley, which is one of the most polluted regions in Europe both in summer and winter (Deserti et al., 2020a); and (2) its high density of vehicular emissions, which is among the highest in Europe (Padoan et al., 2018).

Turin, the capital of the Piedmont region, is a highly industrialized city and densely populated metropolitan area, enjoying a humid subtropical climate. Being known as one of the most technological industrial centers in Europe, this city is located in the western end of the Po Valley, one of the most polluted areas in Europe in the northern part of Italy (Bono et al., 2016; Deserti et al., 2020a). The city suffers from the low dispersion of pollutants, since it is surrounded by the Alps and hills in the North, West, and East, and the wind speed in this area is low. Therefore, the air quality standards are not met in this city (Padoan et al., 2018), and the air quality of Turin is put among the worst in Europe (Sicard et al., 2020).

Research shows that the individual particles of atmospheric PM in Turin are small enough to enter the deep zones of the resident's lungs and cause serious health problems for them (Malandrino et al., 2016). Road traffic is one of the most important sources of pollutant emissions in Turin, owning the following share of the total concentration in the city: 40% of the PM_{10}, 30% of the $PM_{2.5}$, and 75 - 77% of NO_2 (Padoan et al., 2018; Piedmont Region, 2018). The motorization rate in Turin is around 615 per 1000 inhabitants (Kyoto-Club, 2019), leading to a high car density in this city. Therefore, studying the role of traffic in the emission of air pollutants is of high importance in this region.

171

172   2.2.   Data

173   2.2.1.   Traffic flow

174   The traffic flow data considered in the current research refers to two time periods before and

175 during the first COVID-19 lockdown in the city of Turin. The pre-lockdown flow data were taken

176 from the standard hourly mean flows for the year 2018 provided by 5T S.r.l., a company working

177 in the areas related to traffic management in Turin. For the full lockdown period, the real-time

178 traffic flow reported continuously by the real-time traffic monitoring of the 5T website

179 (http://opendata.5t.torino.it/get_fdt) was recorded from March 9th to May 18th, 2020, representing

180 the lockdown period. The recording was conducted with a frequency of 10 minutes and then, mean

181 hourly flow was calculated and used for the analysis. The real-time traffic monitoring network in

182 Turin is based on 31 traffic sensors, however, not all these sensors are properly transmitting data.

183 Therefore, in this study, the analysis is restricted to 15 monitoring points, which effectively report

184 data. Although this traffic monitoring network reports average vehicle speed in every road branch,

185 speed data were not employed in the present study, due to low accuracy. For both the pre-lockdown

186 and full lockdown periods, the available data reported total traffic flow, which was subsequently

187 disaggregated based on circulating vehicle categories.

188

189   2.2.2.   Vehicle type share

190   44 categories of circulating motor vehicles were identified for Turin, considering the class of

191 vehicles in the city and the type of fuel they consume. These categories include busses (consuming

192   diesel, CNG, or electricity), heavy-duty and light-duty vehicles (consuming conventional or Euro

193   1-6 standard petrol), mopeds and motorcycles (consuming conventional or Euro 1- 3^+ standard

194   petrol), and passenger cars (consuming electricity, or any conventional or Euro 1-6 standard diesel,

195   LPG or petrol).

196   The shares of vehicles before the lockdown were estimated based on the total number of

197   registered vehicles in each category in the city extracted from Automobile Club d'Italia

198   (http://www.aci.it/), and the hourly flow extracted from a report by 5T S.r.l. on vehicular mobility

199   in the Piedmont region (5T and Regione_Piemonte, 2019). For the lockdown period, the share of

200   each category in the hourly traffic flow in both working and non-working days was considered in

201   the simulation. Since no data on the share of each of the 44 specified categories in the hourly traffic

202   flow of Turin was available, and this type of data could not be extracted from the recorded traffic

203   flow, an estimation for the share of these vehicles in the traffic flow was made. The data regarding

204   the circulating vehicles was estimated based on the average number of kilometers traveled, and the

205   data regarding the registered vehicles were considered in order to verify the consistency of the

206   disaggregation into categories.

207

208   2.2.3. Emission factors

209   Traffic-induced emissions of NO_x, BaP, $PM_{2.5}$, TSP, and BC were considered in this research.

210   The emission factors of these pollutants, except for BC, for each of the specified 44 categories of

211   vehicles were extracted from the EMEP/EEA air pollutant emission inventory guidebook 2019

212   (http://efdb.apps.eea.europa.eu/). The emission factors for BC were extracted from Krecl et al.

213 (2017) for HDVs, from Ježek et al. (2015) for LDVs and motorbikes, and from Zavala et al. (2017)

214 for buses. Emission factors for electricity consumption were considered zero. These factors are

215 reported in Table A1 in Appendix A with a description of the vehicle categories and the average

216 share of total traffic flow in Turin.

217 Total daily pollutant emission was calculated considering the average hourly share of vehicle

218 flow for each of the 44 categories. For each hour and each road source, daily pollutant emission

219 flow of a generic pollutant P was calculated based on Equation (1),

$$P = \sum_i \sum_j \sum_h F_{i,j,h}\, L_i\, EF_{P,j} \qquad (1)$$

220 where $F_{i,j,h}$ is the traffic flow in road i for vehicle category j at hour h (vehicles h^{-1}); L_i is the

221 length of the road (m), and $EF_{P,j}$ is the average emission factor of the vehicle category j in terms

222 of the pollutant P ($g\ km^{-1}\ vehicle^{-1}$).

223

224 2.2.4. Meteorology

225 Meteorological data were collected from three different meteorological stations in Turin,

226 which are managed by the Local Environmental Protection Agency (ARPA) of the regional air

227 pollution service of Piedmont Region (Figure 1). Hourly observations at the ground level of air

228 humidity, precipitation, solar radiation, temperature, atmospheric pressure, wind speed, and wind

229 direction were collected for this research. The radiosoundings from the WMO station of Milano

230 Linate Airport, which is located approximately 150 km east of Turin, were considered for the

231 collection of the required upper-air data (http://weather.uwyo.edu/). Although this station is rather

232   far from Turin, it is the only source of data in this regard and its soundings can be used considering

233   the relative morphological homogeneity of the western part of the Po Valley (Calori et al., 2006)

234   in which Turin is located. Weather observations were first processed with the CALMET model

235   and then were fed into CALPUFF to conduct the dispersion modeling.

236

237   2.3.   Dispersion modeling

238   In this study, the dispersion of pollutants was simulated using the CALPUFF modeling system.

239   CALPUFF is a Lagrangian multi-layer, multi-species, non-steady-state puff dispersion model that

240   simulates the effects of time- and space-varying meteorological conditions on pollution transport,

241   transformation, and removal (US EPA, 2011). This model simulates puffs of the materials emitted

242   from the modeled sources, reproducing dispersion and transformation processes along the way.

243   Temporal and spatial variations in the meteorological fields are explicitly incorporated in the

244   resulting distribution of puffs throughout a simulation period.

245   With the release of CALPUFF version 7, the linear sources have been replaced with road

246   sources. A new module for representing roadway emissions in dispersion model simulations has

247   been implemented. The new approach simulates line sources such as roadways using the concept

248   of rod-like puffs. Emitting rods follow the same rules as emitting horizontally symmetric Gaussian

249   puffs, but far fewer rods aligned with road segments are needed to emulate the uniform distribution

250   of emissions along a road segment. Near-field "hot spots" can be resolved as well as the drift of

251   pollutants to sensitive areas further away. . For more technical details on the CALPUFF model

252   structure, see the user's guide (Exponent, 2019; US EPA, 2011).

253   Simulations were conducted on a domain of $16.6\ km \times 14.6\ km$, with 10 vertical layers and a

254    $100\ m$ grid step. A total number of 2,484 road sources was considered in the simulation. Figure 1

255   illustrates the modeling domain, the road sources, and the measuring points of traffic flow in the

256   city. A height of $1.5\ m$ was assigned to the emission sources, which are the circulating vehicles

257   categorized in each of the 44 specified classes. The detailed setting of simulation parameters is

258   reported in Table A4 of Appendix A. Due to the high number of emission sources, the

259   computational time required for the detailed simulation was high and therefore, the period of the

260   simulation was restricted to one week, i.e. from April 12nd to April 19th, 2020, with hourly time

261   resolution. No chemical transformation scheme was adopted in the simulations.

262
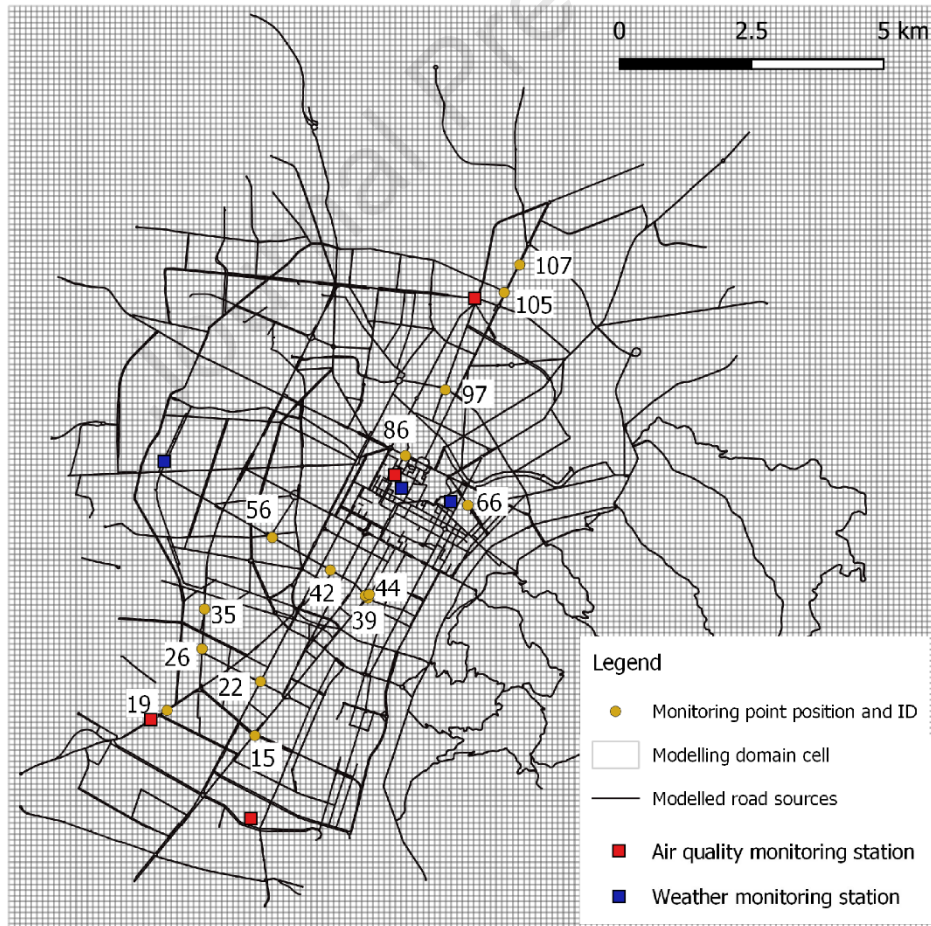
263   *Figure 1. The modeling domain, the road graph, and the location of the monitoring stations.*

264   The output concentrations were averaged over the observation period with the CALPOST

265   processor and represented in the form of maps. Concentration maps of normal days and the

266   COVID-19 country lockdown period were compared, and the reduction of pollutant concentration

267   was calculated. NO_x to NO_2 conversion was modeled in CALPUFF using the MESOPUFF II

268   scheme (Scire et al., 1984). Hourly ozone background concentrations recorded at the Turin

269   Lingotto monitoring station were provided as input to the model.

270

3. Results

271

3.1.   Traffic flow

272

273   Average real-time traffic flow in each hour of the day during the lockdown is compared with

274   the average flow in a normal period, and the flow reduction during the working and non-working

275   days are reported in Tables 2A and 3A in Appendix A, respectively. The same tables also report

276   the average and standard deviation of the traffic flow reduction in each point and each hour of the

277   day. During the working days, 69-88% reduction has been observed in the traffic monitoring points

278   considered. If different hours of the day are examined, traffic flow reduction ranges from 66% to

279   96% during the day. Furthermore, during the non-working days, 74-92% reduction has been

280   perceived in the studied monitoring points. If considering different hours of the day, a range of 49-

281   99% is recognized for the reduction in traffic flow.

282

283   3.2.   Pollutants emission and dispersion

284   The average traffic flow F in each road source during the COVID-19 lockdown days was

285   calculated by scaling the flow in normal days for the average hourly flow reduction observed in

286   the 15 monitoring points reported in Tables A2 and A3 in Appendix A. The results are reported in

287   Table 1 and show an emission reduction between 71.4% (PM$_{2.5}$, working days) and 85.5% (BaP,

288   non-working days).

289

290   *Table 1. Daily pollutant emissions of Turin road traffic in normal days and during the COVID-19 lockdown.*

Pollutant	Daily emission in normal working days (kg/d)	Daily emission during the lockdown working days (kg/d)	Emission Reduction (working days) (%)	Daily emission in normal non-working days (kg/d)	Daily emission during the lockdown non-working days (kg/d)	Emission Reduction (non-working days) (%)
NO$_x$	4,501	1,259	72.0	2,404	383	84.0
BaP	6E-03	1.6E-03	73.3	3.8E-03	5.5E-04	85.5
PM$_{2.5}$	114	32.5	71.4	65	11.1	82.9
TSP	621	174	72.0	337	54.3	83.9
BC	45.4	12.2	73.1	23.7	3.45	85.4

291

292   During the simulation period, there was no rainfall in Turin, except on April 19th, when a total

293   amount of 1.6 mm of rain was recorded. The temperature and solar radiation, and wind distribution

294   during this period are also presented in Figure 2. The wind rose in this figure shows two prevailing

295   wind typologies, which are typical of the area and the period considered. One of them includes

296   moderate winds ($2 - 5\ m/s$) typically occurring during daytime with prevailing direction NE, and

297   the other includes low winds ($0 - 2\ m/s$) typically occurring during nighttime with prevailing

298   direction SE.
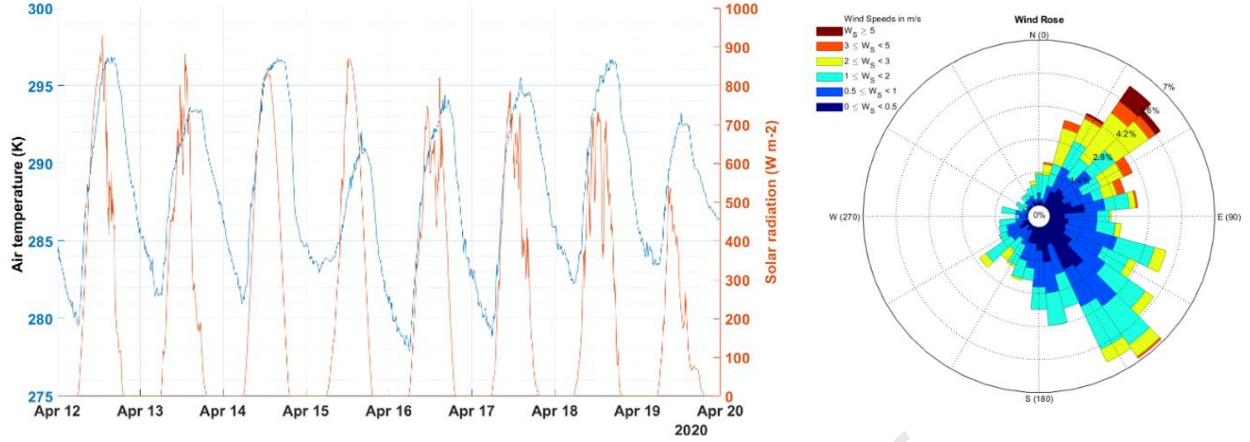
Figure 2. Temperature and solar radiation (left) and wind distribution (right) in Turin during April 12-19, 2020

Figure 3 displays the distribution of the atmospheric stability class, and the height of the mixed layer, and Monin-Obukhov length (L_{mo}) during the simulated period. According to this figure, stable (class F with a share of 33% and E with 12%) and unstable (class B with 32%) conditions were prevailing, while neutral conditions (class C with 12% and D with 5%) were less frequent. This trend is consistent with the general conditions observed during this period. Positive L_{mo} and limited height of the mixed layer on April 14th, 15th, and 17th indicate that stable atmospheric conditions were prevailing on these days, while negative L_{mo} values observed on the other days show the prevalence of unstable conditions, in particular during the daytime.
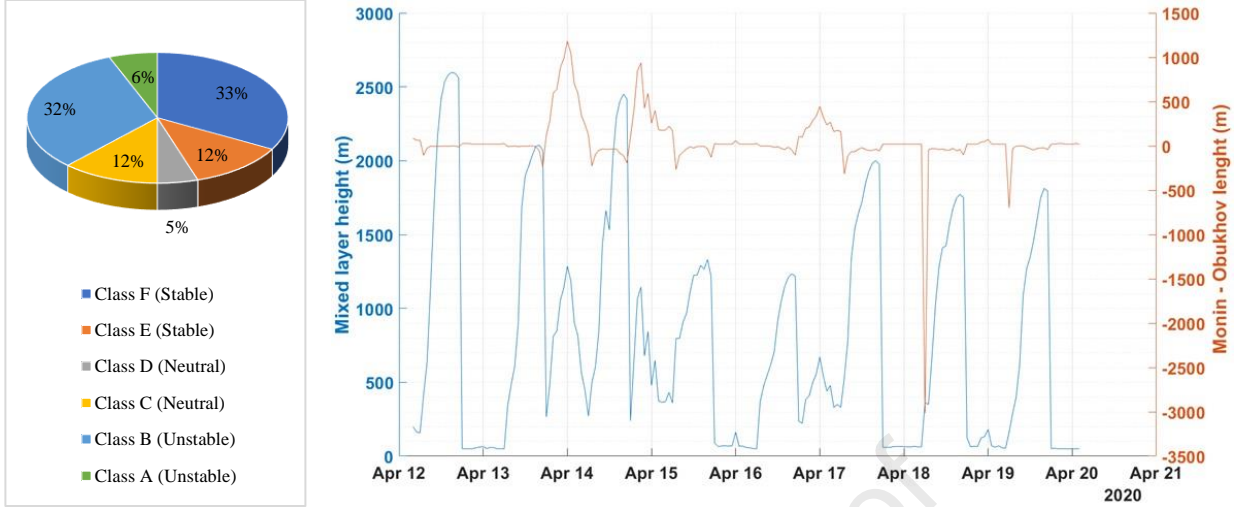
310   *Figure 3. Distribution of the atmospheric stability class (left) and height of the mixed layer and Monin-Obukhov*

311   *length (L_{mo}) (right) in Turin during April 12-19, 2020.*

312

313   Considering the average traffic flow before and during the lockdown, the share of each type of

314   vehicle from the flow, and the meteorological conditions during the studied period, the average

315   pollutant concentration maps are reported in Figure 4 to Figure 8. In these maps, pollutant

316   concentrations generated by urban road traffic on normal days are compared with those generated

317   during one week of the COVID-19 lockdown (April 12nd to April 19th, 2020) based on the same

318   meteorological conditions. The average concentration reduction is reported in Table 2 and finally,

319   presented in Figure 9.

320

321
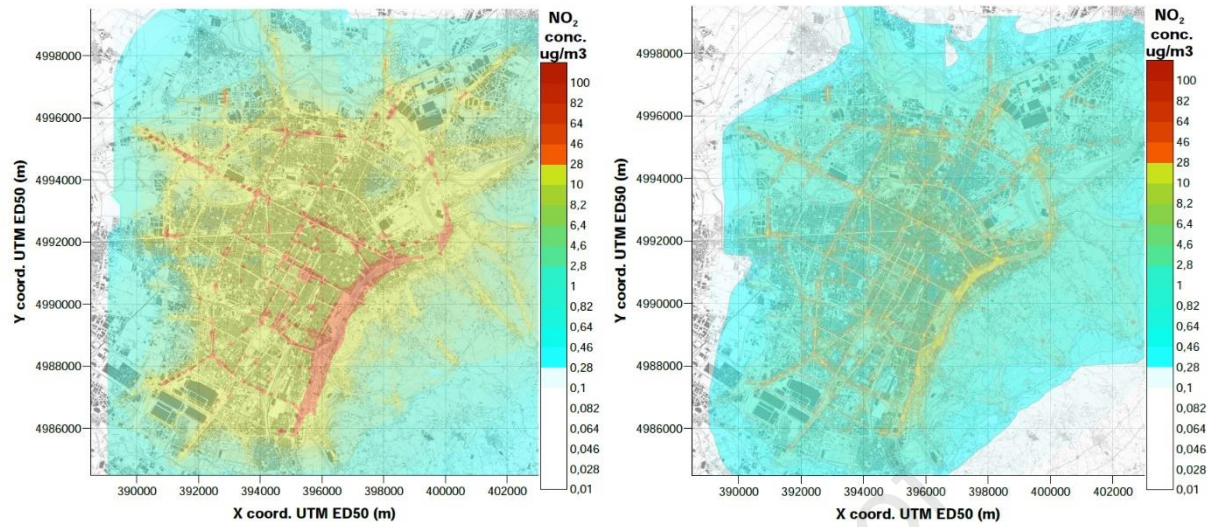
322   *Figure 4. Maps of NO₂ concentration in the Turin area generated by road traffic sources during normal days (left)*

323   *and COVID-19 days (right).*

324
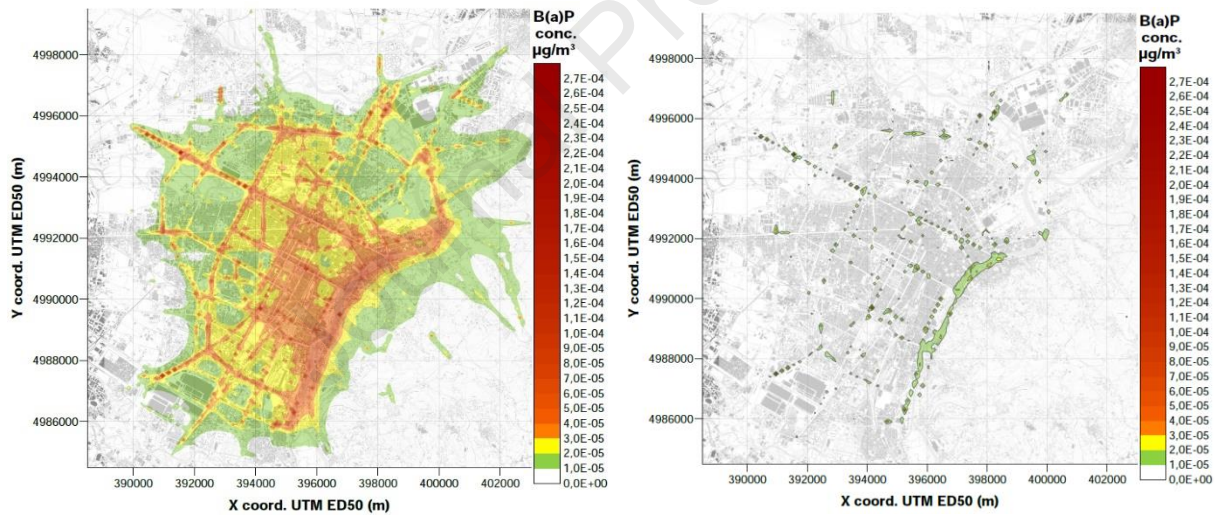
325   *Figure 5. Maps of BaP concentration in the Turin area generated by road traffic sources during normal days (left)*

326   *and COVID-19 days (right).*

327

328
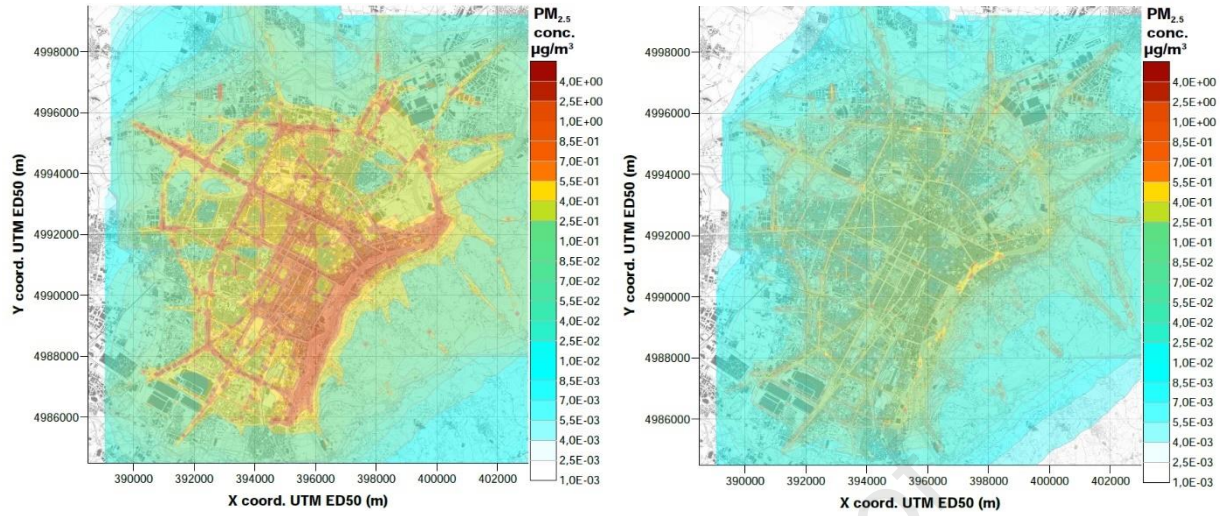
329   *Figure 6. Maps of PM$_{2.5}$ concentration in the Turin area generated by road traffic sources during normal days (left)*

330   *and COVID-19 days (right).*

331
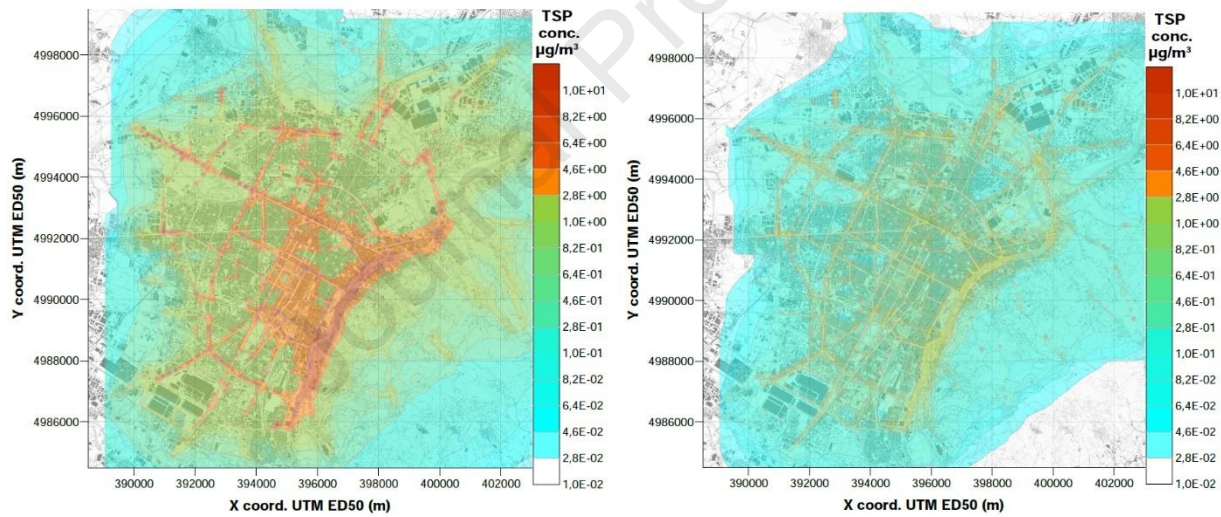
332   *Figure 7. Maps of TSP concentration in the Turin area generated by road traffic sources during normal days (left)*

333   *and COVID-19 days (right).*

334

19

335
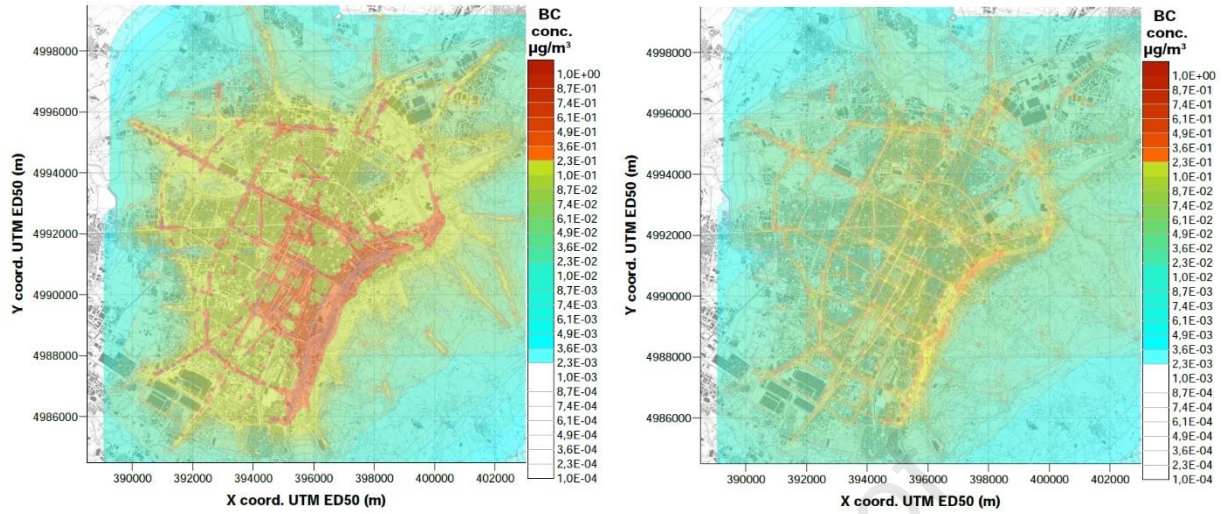
336 *Figure 8. Maps of BC concentration in the Turin area generated by road traffic sources during normal days (left)*

337 *and COVID-19 days (right).*

338

339 *Table 2. Pollutant concentration reduction attributed to traffic in the Turin area during COVID-19 days concerning*

340 *normal days.*

Pollutant	Traffic concentration reduction (%)		
	min	mean	max
NO$_x$	70.7	82.2	87.0
BaP	73.5	83.7	88.1
PM$_{2.5}$	70.0	81.9	86.8
TSP	70.6	82.2	86.9
BC	72.1	83.0	87.9

341

342
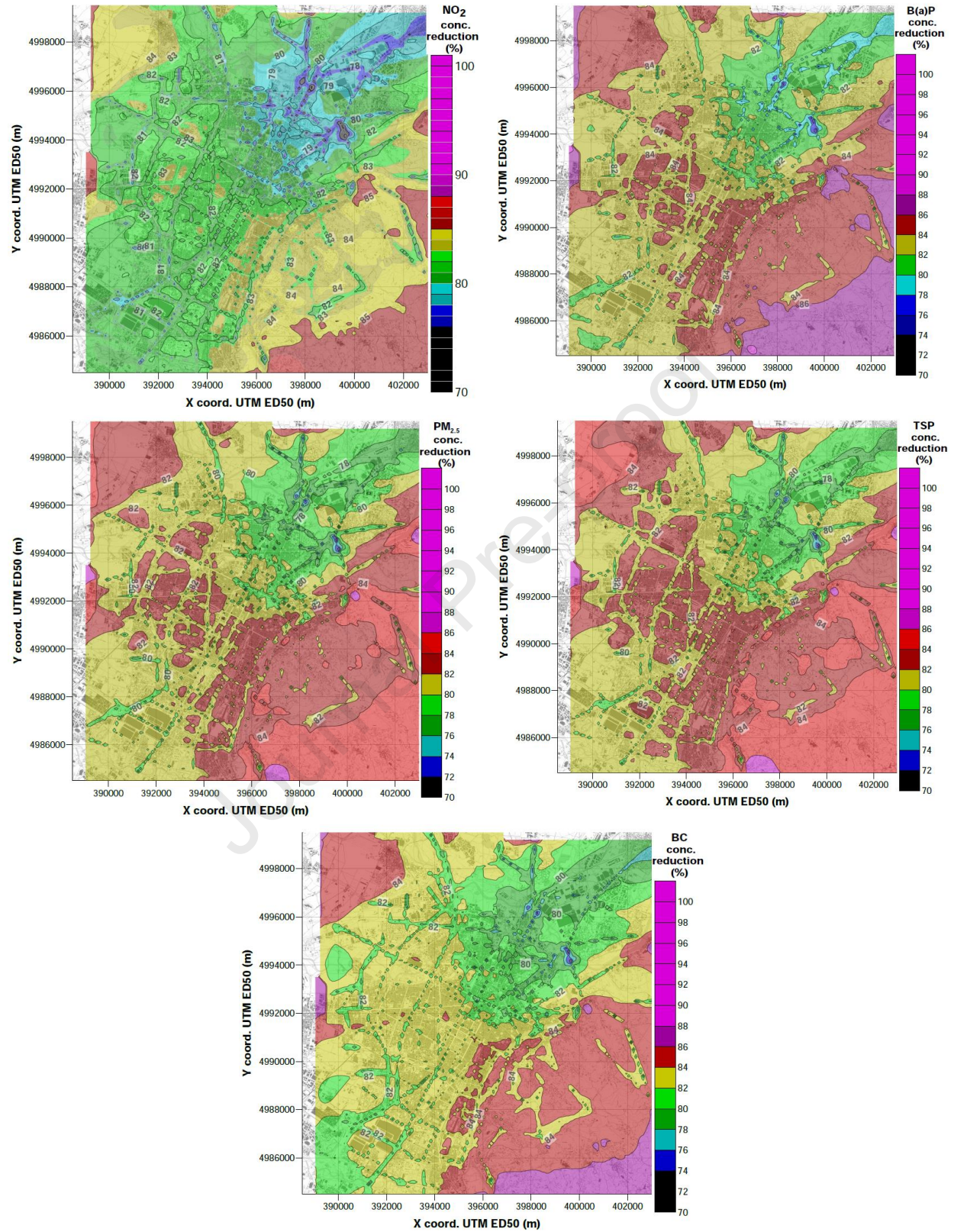
343   *Figure 9. Maps of pollutants concentration reduction during COVID-19 days concerning normal days.*

344

4. Discussion

346   The real-time traffic monitoring in Turin during the whole country lockdown period from

347   March 9th to May 18th, 2020, indicated a significant traffic flow reduction in this metropolitan area.

348   Several companies have published periodic mobility reports based on the location data collected

349   through their services, including Google LLC (2020) and TomTom International BV (2020), or

350   have shared their data through analytical platforms, such as Apple Inc. (2020). The data reported

351   in these reports are consistent with the results obtained in our study, all indicating a flow reduction

352   of around 80%. Tables A2 and A3 presented in the Appendix show that traffic flow had a varying

353   reduction depending on the road and hour of the day. Spatial variations are mainly attributed to

354   the road typology. In general, larger roads (e.g. points 15 and 105), which serve as connections

355   between different areas of the city showed lower reductions, while inner roads serving residential

356   areas (e.g. points 39 and 42) showed larger reductions.

357   The decrease in road mobility resulted in a significant reduction in the emission of the

358   considered pollutants during the studied period in Turin, similar to many other cities in Italy

359   (Gualtieri et al., 2020) and other countries (Chen et al., 2021; Collivignarelli et al., 2021b)

360   reporting significant reductions in the traffic-induced emissions during the lockdown restrictions.

361   Comparing the daily emissions of NO_2, BaP, $PM_{2.5}$, TSP, and BC resulting from the road traffic

362   on normal days and during the COVID-19 lockdown shows that the city experienced more

363   reduction in the emission of air pollutants during non-working days than working days. This

364   difference is mainly due to the activities of some occupations that could not be postponed,

365   canceled, or done from home during the lockdown. Moreover, among the five studied pollutants,

366   BaP had the highest percentage of reduction, while $PM_{2.5}$ showed the lowest percentage of

367   decrease. Different reduction rates may be associated with the difference of emission factors

368   among vehicle typologies. The reduction of traffic flow observed involved mainly a decrease of

369   passenger cars, as this is the most used vehicle typology (81%). For the pollutants whose emission

370   factors for passenger cars have the same order of magnitude as LDVs and HDVs (e.g. BaP, BC),

371   the emission reduction was higher. Conversely, for the pollutants whose emission factors for LDVs

372   and HDVs are higher than those of passenger cars (e.g. NO_x, $PM_{2.5}$), the emission reduction was

373   lower. Although this aspect should be deepened in future studies on traffic flow analysis, the results

374   confirm that the limitation of mobility with private means is of primary importance for

375   administrations (Shams Esfandabadi et al., 2020). These findings are in line with the results of the

376   research conducted by Collivignarelli et al. (2021b), which reports a significant reduction in the

377   concentration of NO_2 during the lockdown period in London, Milan, and Paris and highlight the

378   importance of rethinking vehicles and urban vehicular traffic.

379   As illustrated in the maps of the pollutants concentration reduction in Figure 9 and reported in

380   Table 2, BaP and $PM_{2.5}$ also represent the maximum and minimum percentage of reduction,

381   respectively, in terms of concentration. These results show similar trends for all pollutants, with

382   some minor differences. Regarding $PM_{2.5}$, making a comparison between the results obtained and

383   the existing studies on the COVID-19 lockdown period is difficult. This is because only primary

384   $PM_{2.5}$ emissions were considered in this study. Most of the other studies published recently

385   considered aggregated (primary and secondary) aerosol emissions, highlighting the complexity of

386   the interpretation of $PM_{2.5}$ behavior (Le et al., 2020; Rossi et al., 2020). In general, however, traffic

387   flow reduction was highly reflected in nitrous oxides concentration reduction.

388   Figure 4 to Figure 8 show the spatial distribution of pollutants concentration. The impact is

389   more visible in the proximity of roads, where emissions are generated, but the effects are extended

390   to the whole area. The limited height of sources and the limited dispersion close to the ground are

391   the main factors contributing to the observed trend. These maps also show an uneven distribution

392   of concentration in the area, such that concentrations are higher in the south-eastern part of the

393   town. The presence of a river and reliefs in the eastern part of the city (Figure A1 in Appendix A)

394   contributes to this effect, for two reasons: (1) pollutant dispersion eastwards is limited by the river

395   and reliefs (Ravina et al., 2020a), and (2) traffic is more congested in this area, as the town can

396   only be accessed from north and south. Concentration maps referring to the lockdown period show

397   that the impact, in addition to being reduced, is more limited only to the proximity of the roads.

398   This is an important aspect since consequently, for these pollutants representing a hazard for

399   human health, exposure of the population is limited. Figure 9 shows that the concentration

400   reduction is higher in the north-eastern part of the town. The main reason is that the traffic flow in

401   this area (monitoring points 97, 105, and 107, Table A2 and A3) was less reduced, as mobility in

402   this area is more connected to commercial rather than residential activities.

403   The simulation results for the pollutant NO_2 were compared with the average yearly

404   concentration recorded in four pollutant monitoring stations located in Turin (Rebaudengo,

405   Lingotto, Rubino, and Via Consolata), during the period 2015-2019 and the COVID-19 lockdown

406   period. These monitoring stations record the total ambient concentration of pollutants, which is

407   the result of multiple sources present in the area, as well as the interactions between chemical

408   species and the atmosphere. The comparison is reported in Figure 10. At the Rebaudengo station,

409   the average observed concentration is 65.5 $\mu g/m^3$ and the simulation model shows a concentration

410   of 41.8 $\mu g/m^3$. The average observed concentration in the Via Consolata station is 45.3 $\mu g/m^3$,

411   while the model reports a value of 29.7 $\mu g/m^3$ for this station. Finally, the Lingotto and the Rubino

412   stations have recorded the average observed concentration of 33.0 $\mu g/m^3$ and 31.8 $\mu g/m^3$,

413   respectively, while the simulated model shows 25.6 $\mu g/m^3$ and 15.4 $\mu g/m^3$ for the two stations,

414   respectively.

415   These results are also comparable with the source apportionment data reported in Piedmont

416   Regional Plan for Air Quality (Piedmont Region, 2018). Source apportionment methodology

417   adopted in this document is based on an integration of modeling and analytical techniques. For the

418   modeling source contribution, the methodology adopted is the 3D sensitivity runs / Brute Force

419   Method - BFM. This method involves the creation of a reference simulation (base case) and a

420   suitable number of sensitivity simulations, one for each emission category to be analyzed. The

421   contribution of each category is calculated by analyzing the differences between the results of the

422   sensitivity simulations and those of the base case. Table 3 shows the source apportionment of NO_2

423   concentrations measured on an annual basis at each of the monitoring stations considered.

424   *Table 3. Source apportionment of NO₂ concentrations measured on an annual basis at each of the monitoring*

425   *stations (Piedmont Region, 2018)*

Torino Rebaudengo		Torino Consolata		Torino Lingotto		Torino Rubino	
Emission category	**Share**	**Emission category**	**Share**	**Emission category**	**Share**	**Emission category**	**Share**
Industry	11.2%	Industry	9.1%	Industry	10.8%	Industry	10.7%
Residential heating	9.0%	Residential heating	9.8%	Residential heating	8.8%	Residential heating	8.7%
Road traffic	74.9%	Road traffic	76.5%	Road traffic	76.2%	Road traffic	76.4%
Agriculture	0.6%	Agriculture	0.7%	Agriculture	0.7%	Agriculture	0.7%
Other	4.3%	Other	3.9%	Other	3.5%	Other	3.5%

426

427   In this table, the share of traffic sources from the total NO_2 concentration is reported as 74.9%

428 for Rebaudengo station, 76.5% for Via Consolata station, 76.2% for Lingotto station, and 76.4%

429 for Rubino station. In the simulated concentrations, a share of 63.8% is found at the Rebaudengo

430 station (-11.1% with respect to the inventory data), a share of 65.5% is found at Via della Consolata

431 station (-11.0%), a share of 77.8% is found at the Lingotto station (+1.6%), and a share of 48.4%

432 is found at the Rubino station (-28.0%). Therefore, simulated concentrations of road traffic sources

433 show a similar share with respect to the measured total concentration. The difference does not

434 exceed 11.1% for three over four monitoring stations. The only exception is the Rubino station,

435 where concentrations are underestimated, probably because of the influence of the nearby ring

436 road, which was not included in the study.

437   During the lockdown period, the estimated contribution of traffic emission to the total recorded

438 concentration fell considerably. A share of 22% was found at the Lingotto station, 23% at Via

439 della Consolata station, 31% at Rebaudengo station, and 23% at Rubino station. This reduced share

440 with respect to the normal period, besides the reduced mobility, may also be attributed to the

441 increase of emissions from the residential sector that was confirmed by other studies (Deserti et

442 al., 2020b). Nevertheless, it must be pointed out that the results reported in Figure 10 mainly serve

443 as a piece of indicative information on the validity of the present analysis, which was strictly based

444 on the comparison of primary pollutant emissions, thus does not consider complex aspects of air

445 quality analysis, such as the interaction of multiple emission sources and secondary pollutant

446 transformations.

447
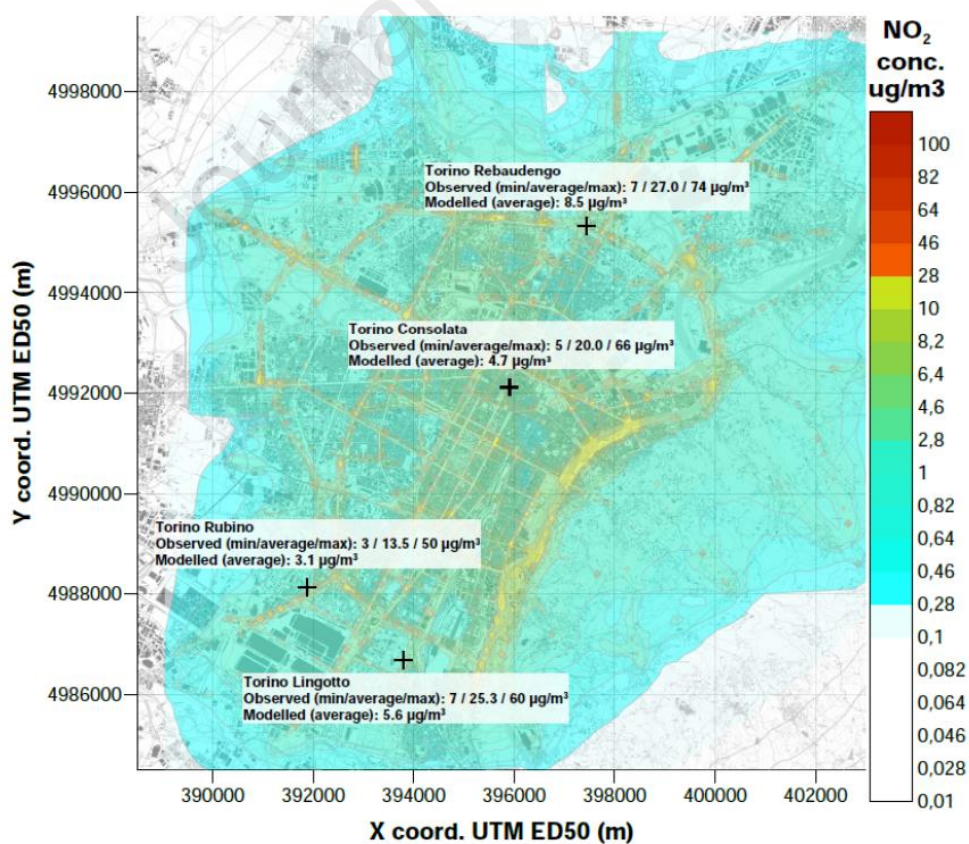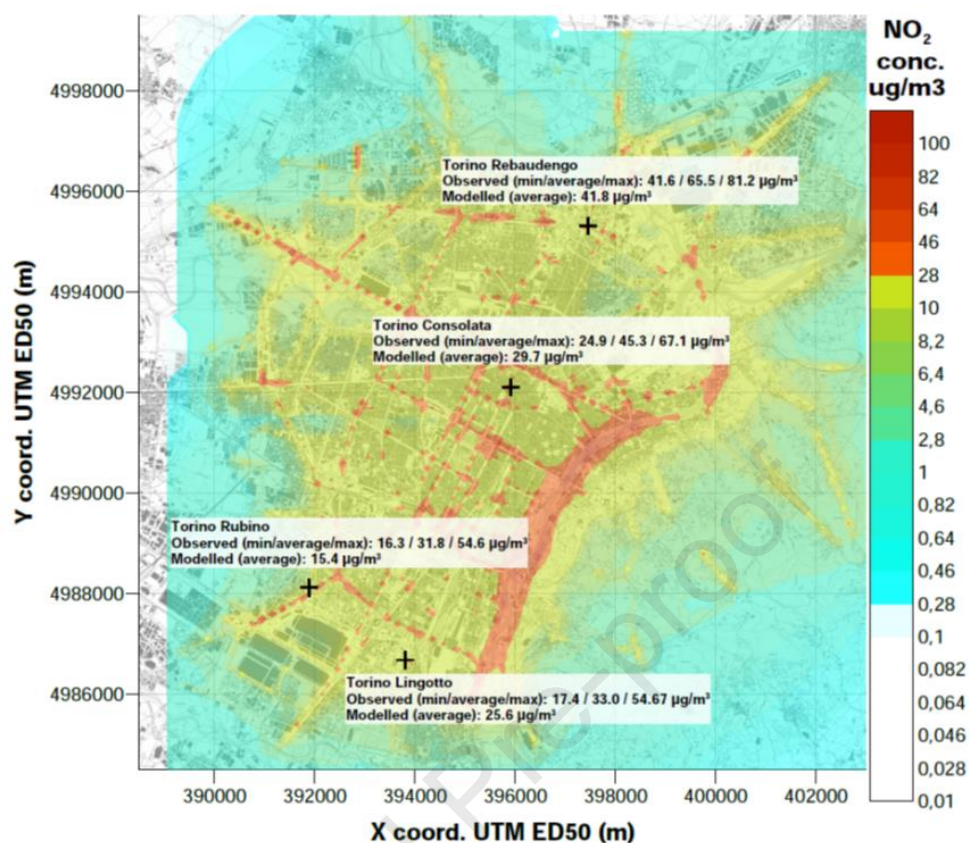
448 *Figure 10. Comparison of the model output for NO_2 with the average yearly concentration recorded in four*

449 *pollutant monitoring stations in Turin (Rebaudengo, Lingotto, Rubino, and Via Consolata) in normal days (above)*

450 *and during the COVID-19 lockdown (below).*

451

452 5. Conclusion

453 The COVID-19 lockdown period, in its tragic nature, was a unique experience to analyze and

454 confirm the role of traffic emissions in urban areas. However, studies applying real quantification

455 of traffic flows during the pandemic lockdown period are scarce and the literature lacks the

456 application of Lagrangian dispersion models to simulate the dispersion of traffic-induced air

457 pollution during the COVID-19 lockdown.

458 In this research, the effect of the full lockdown period on the reduction of NO_2, BaP, $PM_{2.5}$,

459 TSP, and BC emitted from the road mobile sources, including various types of passenger cars,

460 busses, heavy-duty vehicles, light-duty vehicles, mopeds, and motorcycles in Turin, one of the

461 most polluted cities in Italy, was investigated. To do so, the real-time traffic flow of the city during

462 the first lockdown period of the country was recorded and fed into a Lagrangian dispersion model.

463 In the case study analyzed, it was clear that the reduction in vehicular traffic in Turin significantly

464 contributed to the improvement of air quality during the lockdown days. Studying the emission of

465 pollutants in the city during a one-week period in the full lockdown condition indicated a reduction

466 between 71.4% (referring to $PM_{2.5}$ during the working days) and 85.5% (referring to BaP during

467 non-working days). Furthermore, the reduction in the concentration of pollutants in this period

468 varied between 70% (for $PM_{2.5}$) and 88.1% (for BaP).

469   In the concluding remarks, it is necessary to report some important considerations regarding

470   the limitations related to the methodology adopted in the present study. The first is that the present

471   study is based only on the dispersion analysis of primary pollutants and does not consider the

472   totality of the sources present in the area under examination and the chemical transformations

473   occurring between the various species. When considering pollutants that do not tend to undergo

474   secondary transformations, the results reported are fully in line with already published studies

475   (Collivignarelli et al., 2020; Xiang et al., 2020). For PM, it should be noted that the reduction

476   obtained refers only to the primary component. As shown in several other studies (Adams, 2020;

477   Huang et al., 2020; Le et al., 2020; Sreekanth et al., 2021), the overall PM trend, also considering

478   the secondary component, has different results due to multiple factors, which are outside the scope

479   of this study. The second limitation of the method is the application of bulk emission factors, due

480   to the lack of sufficiently accurate data of vehicle speed during the COVID-19 lockdown period.

481   It is not possible to quantify to what extent the change in travel speed resulting from the reduction

482   in traffic flow may have affected vehicle emissions. Considering the method applied, it is clear

483   that in the scenarios examined, the reduction in emissions depended mainly on the reduction in

484   traffic flow on the various sections of the road network and the change in the type of vehicles on

485   the road. The results showed that the reduction of emissions, in addition to the renewal of the

486   vehicle fleet, must be mainly linked to the reduction of movements with private means of transport,

487   given that cars are by far the most present type of vehicles on the road. This consideration is

488   particularly important regarding minor pollutants, such as BaP, and BC, which are majorly

489   dangerous for human health.

490   The subsequent phase of analyzing the spatial distribution of concentrations provided

491   important insights. This research was the first to use a Lagrangian dispersion modeling approach

492   to simulate the dispersion of traffic-induced air pollution during the COVID-19 pandemic. Results

493   showed that in conditions of high vehicular flow, these impacts can extend beyond the proximity

494   of traffic routes and affect pertinential residential areas or parks. On the other hand, a marked

495   reduction in vehicular traffic tends to limit the spatial extension of the impacts. Given the

496   complexity of the subject, these results are recommended to be compared and discussed in future

497   analyses. Confirmation or refutation of these results would bring important implications for air

498   quality and mobility planning in urban areas. Such future studies will bring further knowledge if

499   more detailed and accurate datasets on vehicle flow typology and speed are collected and provided

500   by administrations and stakeholders. Similarly, analyzing different urban areas around the world,

501   in various periods, as well as applying different modeling tools will undoubtedly help increase

502   current knowledge of the topic.

503

References

505   5T, Regione_Piemonte, 2019. Report 2017 sulla mobilità veicolare in Piemonte. Torino, Italy.

506   Abdul-Wahab, S., Al-Rawas, G., Ali, S., Fadlallah, S., Al-Dhamri, H., 2017. Atmospheric dispersion

507   modeling of CO_2 emissions from a cement plant's sources. Clean Technol. Environ. Policy 19,

508   1621–1638. https://doi.org/10.1007/s10098-017-1352-y

509   Abdul-Wahab, S.A., Fadlallah, S.O., 2014. A study of the effects of vehicle emissions on the atmosphere

510   of Sultan Qaboos University in Oman. Atmos. Environ. 98, 158–167.

511   https://doi.org/10.1016/j.atmosenv.2014.08.049

512   Adams, M.D., 2020. Air pollution in Ontario, Canada during the COVID-19 State of Emergency. Sci.

513   Total Environ. 742, 140516. https://doi.org/10.1016/j.scitotenv.2020.140516

514   Ambade, B., Sankar, T.K., Kumar, A., Gautam, A.S., Gautam, S., 2021. COVID-19 lockdowns reduce

515   the Black carbon and polycyclic aromatic hydrocarbons of the Asian atmosphere: source

516   apportionment and health hazard evaluation. Environ. Dev. Sustain. https://doi.org/10.1007/s10668-

517   020-01167-1

518   Apple Inc., 2020. COVID-19 Mobility Trends Reports [WWW Document]. URL

519   https://covid19.apple.com/mobility (accessed 12.23.20).

520   Bono, R., Romanazzi, V., Bellisario, V., Tassinari, R., Trucco, G., Urbino, A., Cassardo, C., Siniscalco,

521   C., Marchetti, P., Marcon, A., 2016. Air pollution, aeroallergens and admissions to pediatric

522   emergency room for respiratory reasons in Turin, northwestern Italy. BMC Public Health 16, 1–11.

523   https://doi.org/10.1186/s12889-016-3376-3

524   Borge, R., Santiago, J.L., de la Paz, D., Martín, F., Domingo, J., Valdés, C., Sánchez, B., Rivas, E.,

525   Rozas, M.T., Lázaro, S., Pérez, J., Fernández, Á., 2018. Corrigendum to "Application of a short

526   term air quality action plan in Madrid (Spain) under a high-pollution episode - Part II: Assessment

527   from multi-scale modelling" [Sci. Total Environ. 635C (2018) 1575-1585]. Sci. Total Environ. 637–

528   638, 1627. https://doi.org/10.1016/j.scitotenv.2018.05.202

529   Brusca, S., Famoso, F., Lanzafame, R., Mauro, S., Messina, M., Strano, S., 2016. PM10 Dispersion

530   Modeling by Means of CFD 3D and Eulerian–Lagrangian Models: Analysis and Comparison with

531   Experiments. Energy Procedia 101, 329–336. https://doi.org/10.1016/j.egypro.2016.11.042

532   Cai, S., Wang, Y., Zhao, B., Wang, S., Chang, X., Hao, J., 2017. The impact of the "Air Pollution

533   Prevention and Control Action Plan" on PM2.5 concentrations in Jing-Jin-Ji region during 2012–

534   2020. Sci. Total Environ. 580, 197–209. https://doi.org/10.1016/j.scitotenv.2016.11.188

535   Calori, G., Clemente, M., De Maria, R., Finardi, S., Lollobrigida, F., Tinarelli, G., 2006. Air quality

536   integrated modelling in Turin urban area. Environ. Model. Softw. 21, 468–476.

537   https://doi.org/10.1016/j.envsoft.2004.06.009

538   Cartenì, A., Di Francesco, L., Martino, M., 2020. How mobility habits influenced the spread of the

539   COVID-19 pandemic: Results from the Italian case study. Sci. Total Environ. 741, 140489.

540   https://doi.org/10.1016/j.scitotenv.2020.140489

541   Cazzolla Gatti, R., Velichevskaya, A., Tateo, A., Amoroso, N., Monaco, A., 2020. Machine learning

542   reveals that prolonged exposure to air pollution is associated with SARS-CoV-2 mortality and

543   infectivity in Italy. Environ. Pollut. 267, 115471. https://doi.org/10.1016/j.envpol.2020.115471

544   Chakraborty, I., Maity, P., 2020. COVID-19 outbreak: Migration, effects on society, global environment

545   and prevention. Sci. Total Environ. 728, 138882. https://doi.org/10.1016/j.scitotenv.2020.138882

546   Charabi, Y., Abdul-Wahab, S., Al-Rawas, G., Al-Wardy, M., Fadlallah, S., 2018. Investigating the impact

547   of monsoon season on the dispersion of pollutants emitted from vehicles: A case study of Salalah

548   City, Sultanate of Oman. Transp. Res. Part D Transp. Environ. 59, 108–120.

549   https://doi.org/10.1016/j.trd.2017.12.019

550   Chen, F., Chen, Z., 2021. Cost of economic growth: Air pollution and health expenditure. Sci. Total

551   Environ. 755, 142543. https://doi.org/10.1016/j.scitotenv.2020.142543

552   Chen, Z., Hao, X., Zhang, X., Chen, F., 2021. Have traffic restrictions improved air quality? A shock

553   from COVID-19. J. Clean. Prod. 279, 123622. https://doi.org/10.1016/j.jclepro.2020.123622

554   Collivignarelli, M.C., Abbà, A., Bertanza, G., Pedrazzani, R., Ricciardi, P., Carnevale Miino, M., 2020.

555   Lockdown for CoViD-2019 in Milan: What are the effects on air quality? Sci. Total Environ. 732,

556   1–9. https://doi.org/10.1016/j.scitotenv.2020.139280

557   Collivignarelli, M.C., Abbà, A., Caccamo, F.M., Bertanza, G., Pedrazzani, R., Baldi, M., Ricciardi, P.,

558   Carnevale Miino, M., 2021a. Can particulate matter be identified as the primary cause of the rapid

559   spread of CoViD-19 in some areas of Northern Italy? Environ. Sci. Pollut. Res. 2.

560   https://doi.org/10.1007/s11356-021-12735-x

561   Collivignarelli, M.C., De Rose, C., Abbà, A., Baldi, M., Bertanza, G., Pedrazzani, R., Sorlini, S.,

562   Carnevale Miino, M., 2021b. Analysis of lockdown for CoViD-19 impact on NO2 in London, Milan

563   and Paris: What lesson can be learnt? Process Saf. Environ. Prot. 146, 952–960.

564   https://doi.org/10.1016/j.psep.2020.12.029

565   Deserti, M., Raffaelli, K., Ramponi, L., Carbonara, C., Agostini, C., Amorati, R., Arvani, B., Giovannini,

566   G., Maccaferri, S., Poluzzi, V., Stortini, M., Trentini, A., Tugnoli, S., Vasconi, M., 2020a. Covid-19

567   and air quality in the Po Valley. Emilia-Romagna Region, Italy.

568   Deserti, M., Raffaelli, K., Ramponi, L., Carbonara, C., Agostini, C., Amorati, R., Arvani, B., Giovannini,

569   G., Maccaferri, S., Poluzzi, V., Stortini, M., Trentini, A., Tugnoli, S., Vasconi, M., 2020b. Report 2

570   COVID-19 studio preliminare degli effetti delle misure COVID-19 sulle emissioni in atmosfera e

571   sulla qualita dell'aria nel bacino padano. Emilia-Romagna Region, Italy.

572   Dettori, M., Deiana, G., Balletto, G., Borruso, G., Murgante, B., Arghittu, A., Azara, A., Castiglia, P.,

573   2020. Air pollutants and risk of death due to COVID-19 in Italy. Environ. Res. 110459.

574   https://doi.org/10.1016/j.envres.2020.110459

575   EPA, 2015. Guidance on the use of models for assessing the impacts of emissions from single sources on

576   the secondarily formed pollutants ozone and PM2.5.

577   Exponent, 2019. CALPUFF Version 7 Users Guide Addendum. Maynard, USA.

578   Gautam, S., 2020. COVID-19: air pollution remains low as people stay at home. Air Qual. Atmos. Heal.

579   13, 853–857. https://doi.org/10.1007/s11869-020-00842-6

580   Google LLC, 2020. COVID-19 community mobility reports [WWW Document]. URL

581   https://www.google.com/covid19/mobility/ (accessed 12.23.20).

582   Griffith, S.M., Huang, W.-S., Lin, C.-C., Chen, Y.-C., Chang, K.-E., Lin, T.-H., Wang, S.-H., Lin, N.-H.,

583   2020. Long-range air pollution transport in East Asia during the first week of the COVID-19

584   lockdown in China. Sci. Total Environ. 741, 140214.

585   https://doi.org/10.1016/j.scitotenv.2020.140214

586   Gross, P.L., Buchanan, N., Sané, S., 2019. Blue skies in the making: Air quality action plans and urban

587   imaginaries in London, Hong Kong, and San Francisco. Energy Res. Soc. Sci. 48, 85–95.

588   https://doi.org/10.1016/j.erss.2018.09.019

589   Gualtieri, G., Brilli, L., Carotenuto, F., Vagnoli, C., Zaldei, A., Gioli, B., 2020. Quantifying road traffic

590   impact on air quality in urban areas: A Covid19-induced lockdown analysis in Italy. Environ. Pollut.

591   267, 115682. https://doi.org/10.1016/j.envpol.2020.115682

592   Gupta, A., Bherwani, H., Gautam, S., Anjum, S., Musugu, K., Kumar, N., Anshul, A., Kumar, R., 2020.

593   Air pollution aggravating COVID-19 lethality? Exploration in Asian cities using statistical models.

594   Environ. Dev. Sustain. https://doi.org/10.1007/s10668-020-00878-9

595   Guttikunda, S.K., Nishadh, K.A., Gota, S., Singh, P., Chanda, A., Jawahar, P., Asundi, J., 2019. Air

596   quality, emissions, and source contributions analysis for the Greater Bengaluru region of India.

597   Atmos. Pollut. Res. 10, 941–953. https://doi.org/10.1016/j.apr.2019.01.002

598   Holnicki, P., Kałuszko, A., Trapp, W., 2016. An urban scale application and validation of the CALPUFF

599   model. Atmos. Pollut. Res. 7, 393–402. https://doi.org/10.1016/j.apr.2015.10.016

600   Huang, X., Ding, A., Gao, J., Zheng, B., Zhou, D., Qi, X., Tang, R., Wang, J., Ren, C., Nie, W., Chi, X.,

601   Xu, Z., Chen, L., Li, Y., Che, F., Pang, N., Wang, H., Tong, D., Qin, W., Cheng, W., Liu, W., Fu,

602   Q., Liu, B., Chai, F., Davis, S.J., Zhang, Q., He, K., 2020. Enhanced secondary pollution offset

603   reduction of primary emissions during COVID-19 lockdown in China. Natl. Sci. Rev.

604   https://doi.org/10.1093/nsr/nwaa137

605   Izquierdo, R., García Dos Santos, S., Borge, R., Paz, D. de la, Sarigiannis, D., Gotti, A., Boldo, E., 2020.

606   Health impact assessment by the implementation of Madrid City air-quality plan in 2020. Environ.

607   Res. 183, 109021. https://doi.org/10.1016/j.envres.2019.109021

608   Ježek, I., Drinovec, L., Ferrero, L., Carriero, M., Močnik, G., 2015. Determination of car on-road black

609   carbon and particle number emission factors and comparison between mobile and stationary

610   measurements. Atmos. Meas. Tech. 8, 43–55. https://doi.org/10.5194/amt-8-43-2015

611   Kesarkar, A.P., Dalvi, M., Kaginalkar, A., Ojha, A., 2007. Coupling of the Weather Research and

612   Forecasting Model with AERMOD for pollutant dispersion modeling. A case study for PM10

613   dispersion over Pune, India. Atmos. Environ. 41, 1976–1988.

614   https://doi.org/10.1016/j.atmosenv.2006.10.042

615   Khan, S., Hassan, Q., 2020. Review of Development in Air Quality Modeling and Air Quality Dispersion

616   Models. J. Environ. Eng. Sci. 1–10. https://doi.org/10.1680/jenes.20.00004

617   Krecl, P., Johansson, C., Targino, A.C., Ström, J., Burman, L., 2017. Trends in black carbon and size-

618   resolved particle number concentrations and vehicle emission factors under real-world conditions.

619   Atmos. Environ. 165, 155–168. https://doi.org/10.1016/j.atmosenv.2017.06.036

620   Kyoto-Club, 2019. Politiche di Mobilità e Qualita dell'aria nelle 14 Citta e aree Metropolitane 2017-2018.

621   Rome, Italy.

622   Le, T., Wang, Y., Liu, L., Yang, J., Yung, Y.L., Li, G., Seinfeld, J.H., 2020. Unexpected air pollution

623   with marked emission reductions during the COVID-19 outbreak in China. Science (80-.). 369,

624   702–706. https://doi.org/10.1126/science.abb7431

625   Liu, F., Wang, M., Zheng, M., 2021. Effects of COVID-19 lockdown on global air quality and health. Sci.

626   Total Environ. 755, 142533. https://doi.org/10.1016/j.scitotenv.2020.142533

627   Liu, Y., Zhao, Y., Lu, W., Wang, H., Huang, Q., 2019. ModOdor: 3D numerical model for dispersion

628   simulation of gaseous contaminants from waste treatment facilities. Environ. Model. Softw. 113, 1–

629   19. https://doi.org/10.1016/j.envsoft.2018.12.001

630   Malandrino, M., Casazza, M., Abollino, O., Minero, C., Maurino, V., 2016. Size resolved metal

631   distribution in the PM matter of the city of Turin (Italy). Chemosphere 147, 477–489.

632   https://doi.org/10.1016/j.chemosphere.2015.12.089

633   Menut, L., Bessagnet, B., Siour, G., Mailler, S., Pennel, R., Cholakian, A., 2020. Impact of lockdown

634 measures to combat Covid-19 on air quality over western Europe. Sci. Total Environ. 741, 140426.

635 https://doi.org/10.1016/j.scitotenv.2020.140426

636 Muhammad, S., Long, X., Salman, M., 2020. COVID-19 pandemic and environmental pollution: A

637 blessing in disguise? Sci. Total Environ. 728, 138820.

638 https://doi.org/10.1016/j.scitotenv.2020.138820

639 Naeger, A.R., Murphy, K., 2020. Impact of COVID-19 Containment Measures on Air Pollution in

640 California. Aerosol Air Qual. Res. 20, 2025–2034. https://doi.org/10.4209/aaqr.2020.05.0227

641 Omidi Khaniabadi, Y., Sicard, P., Taiwo, A.M., De Marco, A., Esmaeili, S., Rashidi, R., 2018. Modeling

642 of particulate matter dispersion from a cement plant: Upwind-downwind case study. J. Environ.

643 Chem. Eng. 6, 3104–3110. https://doi.org/10.1016/j.jece.2018.04.022

644 Padoan, E., Ajmone-Marsan, F., Querol, X., Amato, F., 2018. An empirical model to predict road dust

645 emissions based on pavement and traffic characteristics. Environ. Pollut. 237, 713–720.

646 https://doi.org/10.1016/j.envpol.2017.10.115

647 Panepinto, D., Brizio, E., Genon, G., 2014. Atmospheric pollutants and air quality effects: limitation costs

648 and environmental advantages (a cost–benefit approach). Clean Technol. Environ. Policy 16, 1805–

649 1813. https://doi.org/10.1007/s10098-014-0727-6

650 Piedmont Region, 2018. Air Quality Plan [WWW Document]. URL

651 https://www.regione.piemonte.it/web/temi/ambiente-territorio/ambiente/aria/piano-regionale-

652 qualita-dellaria-prqa (accessed 12.24.20).

653 Pinto, J.A., Kumar, P., Alonso, M.F., Andreão, W.L., Pedruzzi, R., dos Santos, F.S., Moreira, D.M.,

654 Albuquerque, T.T. de A., 2020. Traffic data in air quality modeling: A review of key variables,

655 improvements in results, open problems and challenges in current research. Atmos. Pollut. Res. 11,

656 454–468. https://doi.org/10.1016/j.apr.2019.11.018

657 Ranjbari, M., Shams Esfandabadi, Z., Zanetti, M.C., Scagnelli, S.D., Siebers, P.-O., Aghbashlo, M., Peng,

658   W., Quatraro, F., Tabatabaei, M., 2021. Three pillars of sustainability in the wake of COVID-19: A

659   systematic review and future research agenda for sustainable development. J. Clean. Prod. 297,

660   126660. https://doi.org/10.1016/j.jclepro.2021.126660

661   Ravina, M., Panepinto, D., Zanetti, M., 2020a. District heating networks: an inter-comparison of

662   environmental indicators. Environ. Sci. Pollut. Res. https://doi.org/10.1007/s11356-020-08734-z

663   Ravina, M., Panepinto, D., Zanetti, M., 2019. Air Quality Planning and the Minimization of Negative

664   Externalities. Resources 8, 15. https://doi.org/10.3390/resources8010015

665   Ravina, M., Panepinto, D., Zanetti, M.C., 2020b. Development of the DIDEM Model: Comparative

666   evaluation of CALPUFF and SPRAY dispersion models. Int. J. Environ. Impacts Manag. Mitig.

667   Recover. 3, 1–18. https://doi.org/10.2495/ei-v3-n1-1-18

668   Ravina, M., Panepinto, D., Zanetti, M.C., 2018. DIDEM - An integrated model for comparative health

669   damage costs calculation of air pollution. Atmos. Environ. 173, 81–95.

670   https://doi.org/10.1016/j.atmosenv.2017.11.010

671   Rossi, R., Ceccato, R., Gastaldi, M., 2020. Effect of Road Traffic on Air Pollution. Experimental

672   Evidence from COVID-19 Lockdown. Sustainability 12, 8984. https://doi.org/10.3390/su12218984

673   Saadat, S., Rawtani, D., Hussain, C.M., 2020. Environmental perspective of COVID-19. Sci. Total

674   Environ. 728, 138870. https://doi.org/10.1016/j.scitotenv.2020.138870

675   Scire, J.S., Lurmann, F.W., Bass, A., Hanna, S.R., 1984. User's guide to the MESOPUFF II model and

676   related processor programs, EPA-600/8–84-013. U.S., Environmental Protection Agency, Research

677   Triangle Park.

678   Shahbazi, H., Ganjiazad, R., Hosseini, V., Hamedi, M., 2017. Investigating the influence of traffic

679   emission reduction plans on Tehran air quality using WRF/CAMx modeling tools. Transp. Res. Part

680   D Transp. Environ. 57, 484–495. https://doi.org/10.1016/j.trd.2017.08.001

681   Shahbazi, H., Hosseini, V., 2020. Impact of mobile source emission inventory adjustment on air pollution

682   photochemical model performance. Urban Clim. 32, 100618.

683   https://doi.org/10.1016/j.uclim.2020.100618

684   Shams Esfandabadi, Z., Ravina, M., Diana, M., Zanetti, M.C., 2020. Conceptualizing environmental

685   effects of carsharing services: A system thinking approach. Sci. Total Environ. 745, 141169.

686   https://doi.org/10.1016/j.scitotenv.2020.141169

687   Sharifi, A., Khavarian-Garmsir, A.R., 2020. The COVID-19 pandemic: Impacts on cities and major

688   lessons for urban planning, design, and management. Sci. Total Environ. 749, 142391.

689   https://doi.org/10.1016/j.scitotenv.2020.142391

690   Shen, L., Zhao, T., Wang, H., Liu, J., Bai, Y., Kong, S., Zheng, H., Zhu, Y., Shu, Z., 2021. Importance of

691   meteorology in air pollution events during the city lockdown for COVID-19 in Hubei Province,

692   Central China. Sci. Total Environ. 754, 142227. https://doi.org/10.1016/j.scitotenv.2020.142227

693   Sicard, P., De Marco, A., Agathokleous, E., Feng, Z., Xu, X., Paoletti, E., Rodriguez, J.J.D., Calatayud,

694   V., 2020. Amplified ozone pollution in cities during the COVID-19 lockdown. Sci. Total Environ.

695   735, 139542. https://doi.org/10.1016/j.scitotenv.2020.139542

696   Sivarethinamohan, R., Sujatha, S., Priya, S., Sankaran, Gafoor, A., Rahman, Z., 2020. Impact of air

697   pollution in health and socio-economic aspects: Review on future approach. Mater. Today Proc.

698   https://doi.org/10.1016/j.matpr.2020.08.540

699   Son, J.-Y., Fong, K.C., Heo, S., Kim, H., Lim, C.C., Bell, M.L., 2020. Reductions in mortality resulting

700   from reduced air pollution levels due to COVID-19 mitigation measures. Sci. Total Environ. 744,

701   141012. https://doi.org/10.1016/j.scitotenv.2020.141012

702   Sreekanth, V., Kushwaha, M., Kulkarni, P., Upadhya, A.R., Spandana, B., Prabhu, V., 2021. Impact of

703   COVID-19 lockdown on the fine particulate matter concentration levels: Results from Bengaluru

704   megacity, India. Adv. Sp. Res. 67, 2140–2150. https://doi.org/10.1016/j.asr.2021.01.017

705   Stewart, D.R., Saunders, E., Perea, R.A., Fitzgerald, R., Campbell, D.E., Stockwell, W.R., 2017. Linking

706   Air Quality and Human Health Effects Models: An Application to the Los Angeles Air Basin.

707   Environ. Health Insights 11, 1–13. https://doi.org/10.1177/1178630217737551

708   TomTom International BV, 2020. COVID-19 mobility report [WWW Document]. URL

709   https://www.tomtom.com/covid-19/country/italy (accessed 12.23.20).

710   UN, 2015. Resolution adopted by the General Assembly on 25 September 2015.

711   US EPA, 2011. CALPUFF Modeling System Version 6 User Instructions.

712   Wang, Y., Yuan, Y., Wang, Q., Liu, C.G., Zhi, Q., Cao, J., 2020. Changes in air quality related to the

713   control of coronavirus in China: Implications for traffic and industrial emissions. Sci. Total Environ.

714   731, 139133. https://doi.org/10.1016/j.scitotenv.2020.139133

715   WHO, 2020. WHO Director-General's opening remarks at the media briefing on COVID-19 - 11 March

716   2020 [WWW Document]. URL https://www.who.int/director-general/speeches/detail/who-director-

717   general-s-opening-remarks-at-the-media-briefing-on-covid-19---11-march-2020 (accessed 11.9.20).

718   WHO, 2017. Don't Pollute my future! The impact of the environment on children's health, WHO.

719   Geneva, Switzerland.

720   WHO, 2016. Ambient air pollution: A global assessment of exposure and burden of disease. Geneva,

721   Switzerland.

722   WHO, 2005. Air Quality Guidelines- Global Update 2005. Copenhagen, Denmark.

723   Xiang, J., Austin, E., Gould, T., Larson, T., Shirai, J., Liu, Y., Marshall, J., Seto, E., 2020. Impacts of the

724   COVID-19 responses on traffic-related air pollution in a Northwestern US city. Sci. Total Environ.

725   747, 141325. https://doi.org/10.1016/j.scitotenv.2020.141325

726   Zangari, S., Hill, D.T., Charette, A.T., Mirowsky, J.E., 2020. Air quality changes in New York City

727   during the COVID-19 pandemic. Sci. Total Environ. 742, 140496.

728   https://doi.org/10.1016/j.scitotenv.2020.140496

729 Zavala, M., Molina, L.T., Yacovitch, T.I., Fortner, E.C., Roscioli, J.R., Floerchinger, C., Herndon, S.C.,

730 Kolb, C.E., Knighton, W.B., Paramo, V.H., Zirath, S., Mejía, J.A., Jazcilevich, A., 2017. Emission

731 factors of black carbon and co-pollutants from diesel vehicles in Mexico City. Atmos. Chem. Phys.

732 17, 15293–15305. https://doi.org/10.5194/acp-17-15293-2017

733

Appendix A. Supplementary data

Table A1. Vehicle categories, the share of total vehicle flow in Turin, and related average emission factors

Category	Technology	Fuel	Abatement	Share from the total vehicle flow (%)	Emission factors (g/km)				
					NO_x	BaP	$PM_{2.5}$	TSP	BC
1	Buses	Diesel	Urban Buses Standard - Euro V - 2008	0.29%	3.09	9.0E-07	0.046	0.498	0.001
2	Buses	CNG	Urban CNG Buses - EEV	0.04%	2.5	0	0.005	0.163	0
3	Heavy-duty vehicles	Diesel	Diesel 7.5 - 16 t - Conventional	0.46%	8.92	9.0E-07	0.334	0.379	0.205
4	Heavy-duty vehicles	Diesel	Diesel 7.5 - 16 t - Euro I - 91/542/EEC I	0.18%	5.31	9.0E-07	0.201	0.379	0.199
5	Heavy-duty vehicles	Diesel	Diesel 7.5 - 16 t - Euro II - 91/542/EEC II	0.37%	5.5	9.0E-07	0.104	0.379	0.100
6	Heavy-duty vehicles	Diesel	Diesel 7.5 - 16 t - Euro III - 2000	0.55%	4.3	9.0E-07	0.088	0.379	0.090
7	Heavy-duty vehicles	Diesel	Diesel 7.5 - 16 t - Euro IV - 2005	0.67%	2.65	9.0E-07	0.016	0.379	0.016
8	Heavy-duty vehicles	Diesel	Diesel 7.5 - 16 t - Euro V - 2008	0.59%	1.51	9.0E-07	0.016	0.379	0.016
9	Heavy-duty vehicles	Diesel	Diesel 7.5 - 16 t - Euro VI	0.81%	0.291	9.0E-07	0.001	0.379	0.016
10	Light commercial vehicles	Petrol	Diesel - Conventional	0.46%	1.66	2.9E-06	0.179	0.179	0.003
11	Light commercial vehicles	Petrol	Diesel - Euro 1 - 93/59/EEC	0.18%	1.22	6.3E-07	0.117	0.179	0.002
12	Light commercial vehicles	Petrol	Diesel - Euro 2 - 96/69/EEC	0.37%	1.22	6.3E-07	0.117	0.179	0.001
13	Light commercial vehicles	Petrol	Diesel - Euro 3 - 98/69/EC I	0.55%	1.03	6.3E-07	0.078	0.179	0.001
14	Light commercial vehicles	Petrol	Diesel - Euro 4 - 98/69/EC II	0.67%	0.831	6.3E-07	0.041	0.179	0.001
15	Light commercial vehicles	Petrol	Diesel - Euro 5 – EC 715/2007	0.59%	1.15	6.3E-07	0.001	0.179	0.001
16	Light commercial vehicles	Petrol	Diesel - Euro 6 up to 2017	0.81%	0.96	6.3E-07	0.001	0.179	0.001
17	Mopeds and motorcycles	Petrol	2-stroke - Mop - Higher than Euro 3	0.96%	0.25	2.3E-06	0.018	0.091	0.004
18	Mopeds and motorcycles	Petrol	2-stroke - Mop - Euro 3	3.60%	0.25	2.3E-06	0.018	0.091	0.004
19	Mopeds and motorcycles	Petrol	2-stroke - Mop - Euro 2	1.54%	0.25	2.3E-06	0.026	0.091	0.004

No.	Category	Fuel	Description						
20	Mopeds and motorcycles	Petrol	2-stroke - Mop - Euro 1	1.69%	0.25	2.3E-06	0.045	0.091	0.004
21	Mopeds and motorcycles	Petrol	2-stroke - Conventional	3.25%	0.25	2.3E-06	0.091	0.091	0.004
22	Passenger Cars	Diesel	Diesel Medium - Conventional	1.03%	0.546	1.7E-06	0.099	0.099	0.099
23	Passenger Cars	Diesel	Diesel Medium - Euro 1 - 91/441/EEC	0.22%	0.69	1.7E-06	0.084	0.099	0.008
24	Passenger Cars	Diesel	Diesel Medium - Euro 2 - 94/12/EEC	0.84%	0.716	1.7E-06	0.055	0.099	0.042
25	Passenger Cars	Diesel	Diesel Medium - Euro 3 - 98/69/EC I	2.98%	0.773	1.7E-06	0.039	0.099	0.039
26	Passenger Cars	Diesel	Diesel Medium - Euro 4 - 98/69/EC II	6.01%	0.58	1.7E-06	0.031	0.099	0.012
27	Passenger Cars	Diesel	Diesel Medium - Euro 5 – EC 715/2007	6.14%	0.55	1.7E-06	0.002	0.099	0.011
28	Passenger Cars	Diesel	Diesel Medium - Euro 6 up to 2016	11.09%	0.45	1.7E-06	0.002	0.099	0.000
29	Passenger Cars	LPG	LPG - Conventional	0.39%	2.36	1.0E-08	0.002	0.033	0.001
30	Passenger Cars	LPG	LPG - Euro 1 - 91/441/EEC	0.11%	0.414	1.0E-08	0.002	0.033	0
31	Passenger Cars	LPG	LPG - Euro 2 - 94/12/EEC	0.35%	0.18	1.0E-08	0.002	0.033	0
32	Passenger Cars	LPG	LPG - Euro 3 - 98/69/EC I	0.32%	0.09	1.0E-08	0.001	0.033	0
33	Passenger Cars	LPG	LPG - Euro 4 - 98/69/EC II	3.27%	0.056	1.0E-08	0.001	0.033	0
34	Passenger Cars	LPG	LPG - Euro 5 – EC 715/2007	1.85%	0.056	1.0E-08	0.001	0.033	0
35	Passenger Cars	LPG	LPG - Euro 6 – EC 715/2007	3.82%	0.056	1.0E-08	0.001	0.033	0
36	Passenger Cars	Petrol	Petrol Medium - ECE 15/04	5.67%	2.66	4.8E-07	0.002	0.035	0.002
37	Passenger Cars	Petrol	Petrol Medium - Euro 1 - 91/441/EEC	1.11%	0.485	3.2E-07	0.002	0.035	0.002
38	Passenger Cars	Petrol	Petrol Medium - Euro 2 - 94/12/EEC	4.03%	0.255	3.2E-07	0.002	0.035	0.002
39	Passenger Cars	Petrol	Petrol Medium - Euro 3 - 98/69/EC I	4.79%	0.097	3.2E-07	0.001	0.035	0.001
40	Passenger Cars	Petrol	Petrol Medium - Euro 4 - 98/69/EC II	10.02%	0.061	3.2E-07	0.001	0.035	0.001
41	Passenger Cars	Petrol	Petrol Medium - Euro 5 – EC 715/2007	4.86%	0.061	3.2E-07	0.001	0.035	0.001
42	Passenger Cars	Petrol	Petrol Medium - Euro 6 up to 2016	11.33%	0.061	3.2E-07	0.001	0.035	0.001
43	Buses	Electricity		0.01%	0	0.0E+00	0.000	0.154	0
44	Passenger Cars	Electricity		1.15%	0	0.0E+00	0.000	0.033	0

Table A2. Traffic flow reduction in the traffic monitoring points (working days).

Hour of the day	Point ID 15	19	22	26	35	39	42	44	49	56	66	86	97	105	107	Mean	Std. dev.
Coord. (N, W)	45.0326, 7.6466	45.0364, 7.6266	45.0413, 7.6477	45.0463, 7.6343	45.0527, 7.6347	45.0550, 7.6717	45.0553, 7.6711	45.0555, 7.6770	45.0593, 7.6631	45.0645, 7.6498	45.0702, 7.6640	45.0780, 7.6797	45.0887, 7.6885	45.1045, 7.7015	45.1090, 7.7049		
00:00 – 00:59	92%	90%	100%	95%	93%	100%	100%	100%	95%	100%	100%	100%	93%	89%	90%	**96%**	4%
1:00 – 01:59	100%	90%	100%	90%	85%	100%	100%	100%	100%	100%	100%	100%	85%	92%	91%	**96%**	6%
2:00 – 02:59	100%	89%	100%	100%	100%	100%	100%	100%	100%	100%	100%	100%	72%	87%	86%	**96%**	8%
3:00 – 03:59	100%	79%	100%	82%	100%	100%	100%	100%	100%	100%	100%	100%	100%	80%	82%	**95%**	9%
4:00 – 04:59	64%	80%	100%	76%	84%	100%	100%	71%	100%	100%	100%	100%	73%	67%	78%	**86%**	14%
5:00 – 05:59	44%	60%	86%	71%	72%	67%	75%	71%	86%	70%	72%	76%	71%	60%	76%	**70%**	10%
6:00 – 06:59	48%	60%	76%	68%	59%	67%	76%	72%	76%	68%	65%	68%	64%	60%	63%	**66%**	7%
7:00 – 07:59	34%	75%	85%	81%	77%	76%	79%	83%	84%	80%	76%	75%	77%	73%	73%	**75%**	12%
8:00 – 08:59	55%	74%	78%	80%	75%	78%	78%	74%	83%	74%	77%	73%	74%	73%	76%	**75%**	6%
9:00 – 09:59	60%	77%	80%	79%	71%	80%	78%	77%	81%	77%	80%	79%	77%	72%	77%	**76%**	5%
10:00 – 10:59	57%	73%	82%	77%	66%	79%	77%	77%	79%	77%	77%	78%	75%	71%	71%	**74%**	6%
11:00 – 11:59	61%	74%	84%	76%	65%	77%	77%	77%	75%	75%	76%	78%	73%	69%	70%	**74%**	5%
12:00 – 12:59	55%	73%	84%	75%	66%	77%	73%	77%	72%	77%	75%	77%	70%	69%	69%	**73%**	6%
13:00 – 13:59	51%	72%	81%	74%	66%	77%	75%	75%	71%	74%	77%	75%	70%	68%	68%	**72%**	7%
14:00 – 14:59	57%	76%	81%	74%	68%	79%	78%	81%	79%	79%	77%	79%	74%	72%	70%	**75%**	6%
15:00 – 15:59	60%	77%	83%	77%	71%	80%	79%	82%	80%	80%	80%	80%	76%	73%	73%	**77%**	6%
16:00 – 16:59	65%	76%	86%	79%	74%	84%	83%	83%	78%	82%	82%	82%	76%	73%	76%	**79%**	5%
17:00 – 17:59	71%	77%	85%	78%	74%	84%	82%	84%	77%	83%	79%	80%	76%	74%	78%	**79%**	4%
18:00 – 18:59	77%	80%	87%	82%	78%	83%	84%	85%	76%	83%	82%	81%	77%	77%	81%	**81%**	3%
19:00 – 19:59	74%	84%	87%	85%	82%	87%	83%	89%	81%	85%	84%	86%	79%	81%	84%	**83%**	4%
20:00 – 20:59	76%	86%	92%	85%	81%	88%	86%	89%	87%	86%	85%	90%	82%	85%	82%	**85%**	4%
21:00 – 21:59	76%	85%	92%	86%	80%	85%	86%	85%	85%	84%	90%	89%	82%	82%	81%	**84%**	4%
22:00 – 22:59	79%	89%	92%	85%	82%	91%	90%	94%	87%	91%	89%	91%	84%	83%	79%	**87%**	5%
23:00 – 00:59	90%	90%	96%	92%	89%	96%	96%	93%	94%	95%	94%	95%	91%	85%	91%	**92%**	3%
Average	**69%**	**78%**	**88%**	**81%**	**77%**	**85%**	**85%**	**84%**	**84%**	**84%**	**84%**	**85%**	**78%**	**76%**	**78%**	**81%**	5%
Std. dev.	18%	8%	8%	8%	11%	10%	9%	10%	9%	10%	10%	10%	8%	9%	8%		

Table A3. Traffic flow reduction in the traffic monitoring points (non-working days).

Hour of the day	Point ID 15	19	22	26	35	39	42	44	49	56	66	86	97	105	107	Mean	Std. dev.
Coord. (N W)	45.0326, 7.6466	45.0364, 7.6266	45.0413, 7.6477	45.0463, 7.6343	45.0527, 7.6347	45.0550, 7.6717	45.0553, 7.6711	45.0555, 7.6720	45.0593, 7.6631	45.0645, 7.6498	45.0702, 7.6940	45.0780, 7.6797	45.0887, 7.6885	45.1045, 7.7015	45.1090, 7.7049		
00:00 – 00:59	94%	96%	100%	97%	97%	100%	100%	100%	100%	100%	100%	98%	96%	93%	97%	**98%**	2%
1:00 – 01:59	100%	97%	100%	100%	100%	100%	100%	100%	100%	100%	100%	100%	95%	97%	97%	**99%**	2%
2:00 – 02:59	100%	96%	100%	100%	100%	100%	100%	100%	100%	100%	100%	100%	100%	95%	96%	**99%**	2%
3:00 – 03:59	100%	94%	100%	96%	100%	100%	100%	100%	100%	100%	100%	100%	100%	94%	94%	**99%**	2%
4:00 – 04:59	100%	91%	100%	100%	100%	100%	100%	100%	100%	100%	100%	100%	100%	82%	100%	**98%**	5%
5:00 – 05:59	48%	61%	93%	59%	50%	84%	100%	71%	83%	80%	79%	84%	78%	72%	72%	**74%**	14%
6:00 – 06:59	0%	35%	71%	45%	15%	49%	80%	71%	71%	55%	45%	47%	55%	41%	56%	**49%**	21%
7:00 – 07:59	35%	51%	80%	63%	51%	72%	47%	77%	55%	61%	65%	45%	68%	51%	49%	**58%**	12%
8:00 – 08:59	58%	68%	82%	75%	69%	74%	76%	82%	72%	68%	67%	73%	76%	67%	71%	**72%**	6%
9:00 – 09:59	64%	78%	93%	85%	78%	79%	78%	77%	82%	80%	80%	84%	84%	80%	80%	**80%**	6%
10:00 – 10:59	75%	80%	93%	85%	79%	84%	78%	88%	85%	86%	86%	87%	85%	82%	85%	**84%**	4%
11:00 – 11:59	78%	85%	91%	85%	79%	81%	78%	85%	82%	80%	81%	86%	81%	85%	84%	**83%**	3%
12:00 – 12:59	76%	86%	91%	84%	81%	82%	82%	86%	81%	81%	85%	86%	81%	85%	82%	**83%**	3%
13:00 – 13:59	61%	82%	88%	78%	70%	79%	77%	82%	72%	78%	76%	81%	71%	80%	72%	**77%**	6%
14:00 – 14:59	54%	77%	90%	79%	71%	79%	80%	88%	80%	80%	81%	85%	75%	80%	79%	**79%**	8%
15:00 – 15:59	80%	84%	92%	88%	77%	87%	84%	88%	88%	86%	89%	91%	83%	88%	85%	**86%**	4%
16:00 – 16:59	85%	90%	92%	87%	82%	88%	90%	89%	91%	87%	90%	93%	85%	87%	88%	**88%**	3%
17:00 – 17:59	87%	90%	92%	86%	78%	87%	88%	92%	90%	87%	89%	93%	85%	88%	89%	**88%**	4%
18:00 – 18:59	86%	90%	93%	87%	81%	87%	88%	91%	91%	87%	88%	92%	84%	89%	89%	**88%**	3%
19:00 – 19:59	85%	91%	94%	85%	81%	87%	88%	90%	87%	87%	87%	92%	84%	90%	88%	**88%**	3%
20:00 – 20:59	81%	89%	94%	85%	80%	87%	85%	88%	86%	82%	84%	91%	82%	90%	85%	**86%**	4%
21:00 – 21:59	78%	87%	91%	85%	79%	81%	85%	89%	83%	81%	88%	90%	83%	89%	81%	**85%**	4%
22:00 – 22:59	75%	89%	93%	86%	84%	84%	90%	94%	89%	89%	94%	91%	82%	87%	85%	**87%**	5%
23:00 – 00:59	87%	92%	98%	94%	87%	94%	95%	92%	93%	94%	93%	94%	90%	91%	90%	**92%**	3%
Average	**74%**	**82%**	**92%**	**84%**	**78%**	**85%**	**86%**	**88%**	**86%**	**85%**	**85%**	**87%**	**83%**	**83%**	**83%**	**84%**	4%
Std. dev.	23%	15%	7%	13%	19%	11%	12%	9%	11%	12%	13%	14%	11%	13%	12%		

Table A4. Setting of dispersion simulation parameters.

| Parameter	Description	Setting
MGAUSS	Vertical distribution used in the near field	Gaussian
MCTADJ	Terrain adjustment method	Partial plume path adjustment
MSPLIT	Puff splitting	allowed
MCHEM	Chemical mechanism	Transformation rates computed internally (MESOPUFF II scheme)
MDRY	Dry deposition modeled	Not modelled
MDISP	Method used to compute dispersion coefficients	Dispersion coefficients from internally calculated sigma v, sigma w using micrometeorological variables (u*, w*, L, etc.)
MTAULY	Method used for Lagrangian timescale for Sigma-y	Draxler default 617.284 (s)
MCTURB	Method used to compute turbulence sigma-v & sigma-w using micrometeorological variables	Standard CALPUFF subroutines
MBCON	Boundary conditions (concentration)	Not modelled
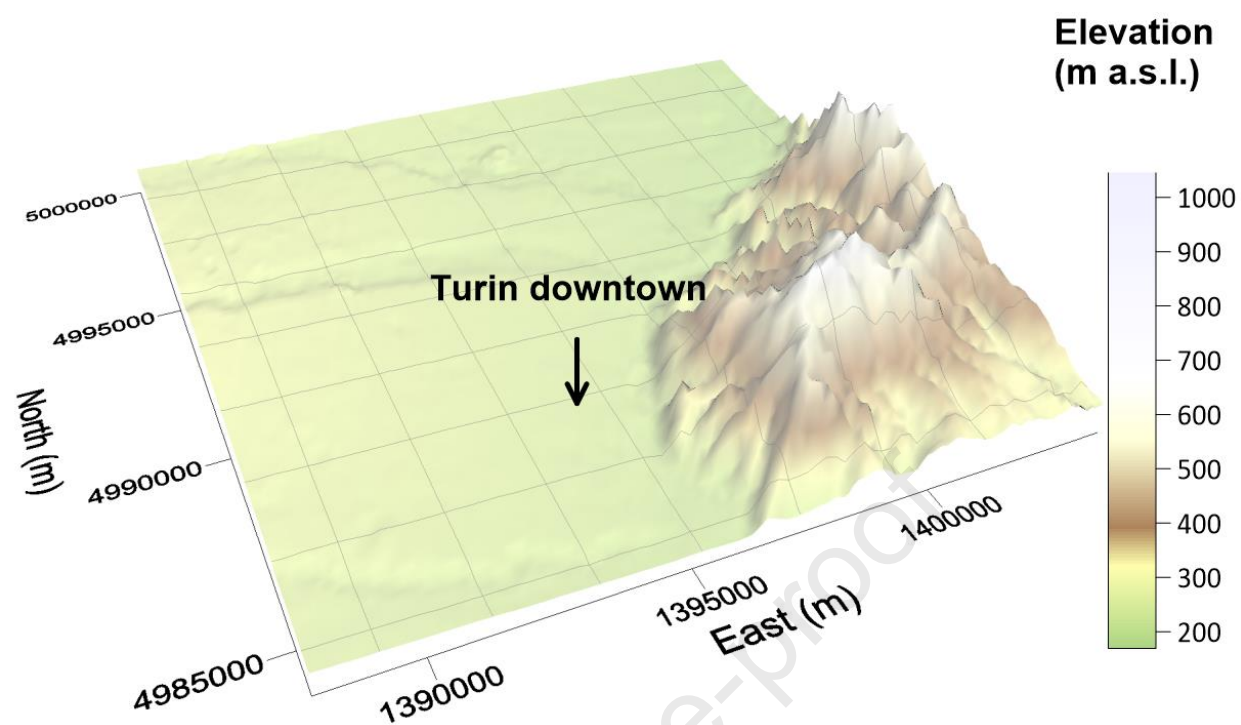
Figure A1. Topography of the modelling domain.